

Supporting Information

.....

**Bis-imidazolium linked Covalent Organic Network Effectively Remove
Arsenate from Water and Wastewater Containing Phosphates**

Gunanka Hazarika,^a Debasis Manna*^{ab}

^aCentre for the Environment, Indian Institute of Technology Guwahati, Assam-781039, India

^bDepartment of Chemistry, Indian Institute of Technology Guwahati

Assam-781039, India, E-mail: dmanna@iitg.ac.in.

Table of Contents

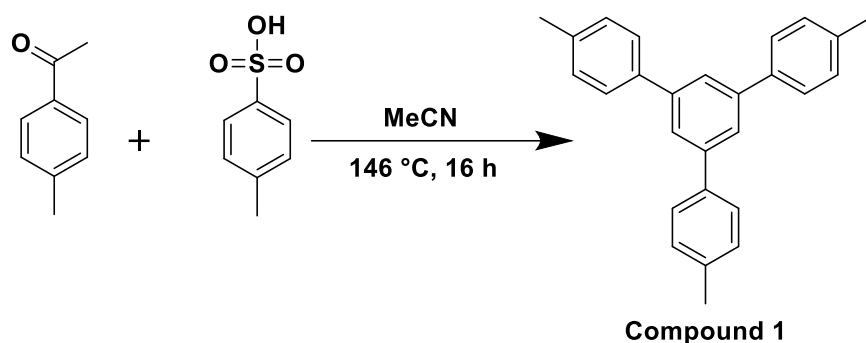
Sl. No.	Description	Page No.
1	General information	S3
2	Synthesis and characterization	S3 – S5
3	Experimental methods	S6 – S13
4	Adsorption study	S13 – S26
5	Regeneration analyses of IC-CON	S26 – S29
6	Arsenate and phosphate desorption kinetics	S29 – S31
7	Morphological analysis after arsenate and phosphate ions adsorption	S31 – S33
8	Mechanism for arsenate and phosphate adsorption	S33 – S34
9	Dynamic adsorption column experiment	S35 – S36
10	Comparison of arsenate adsorption capacity by recently reported materials	S37 – S38
11	Comparison of phosphate adsorption capacity by recently reported materials	S38 – S40
12	^1H NMR and ^{13}C NMR spectra of synthesized compounds	S41 – S43
13	References	S44 – S46

General information:

All reagents were purchased from Sigma-Aldrich, Merck, Himedia and other commercial sources and used directly without further purification. The column chromatography was performed using 60–120 mesh silica gels. Reactions were monitored by thin-layer chromatography (TLC) on silica gel 60 F254 (0.25 mm). The ^1H NMR and ^{13}C NMR were recorded at 400 or 600 and 100 or 151 MHz with Varian AS400 spectrometer and Bruker spectrometer, respectively. The chemical shifts were reported in parts per million (δ) using DMSO-d_6 , CDCl_3 as internal solvent. The coupling constant (J values) and chemical shifts (δ_{ppm}) were reported in Hertz (Hz) and parts per million (ppm), respectively, downfield from tetramethylsilane using residual chloroform ($d = 7.24$ for ^1H NMR, $d = 77.23$ for ^{13}C NMR) as an internal standard. Multiplicities are reported as follows: s (singlet), d (doublet), t (triplet), m (multiplet), and br (broadened). High-resolution mass spectra (HRMS) were recorded at Agilent Q-TOF mass spectrometer with Z-spray source using built-in software for analysis of the recorded data. The maximum number of experiments was repeated three times, and the mean value obtained for each case was reported. The error bars in the figures represent the standard deviations of these repetitions. In the Fourier Transform Infrared Spectroscopy (FT-IR) analysis, sharp peaks are labelled as "S," and broad peaks are marked as "br." The arsenate and phosphate adsorption experimental procedures involve conducting batch experiments in 10 mL glass vials.

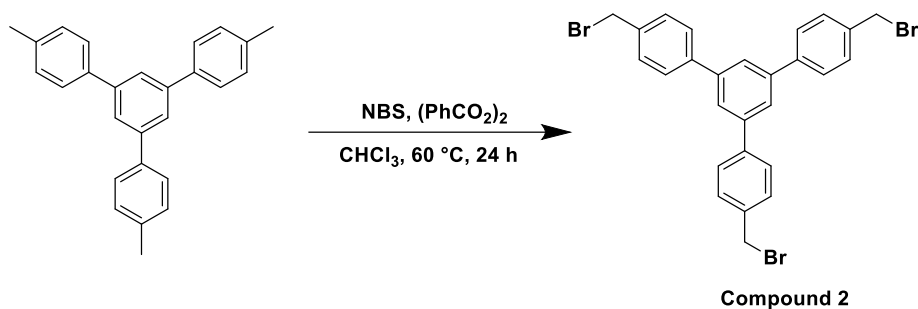
Synthesis and characterization:

Synthesis of 4,4'-dimethyl-5'-(p-tolyl)-1,1':3',1''-terphenyl (compound 1) —1-(p-tolyl)ethan-1-one (500 mg, 3.72 mmol, 1.0 eq.) and p-Toluenesulfonic acid (64.05 mg, 0.37 mmol, 0.1 eq.) were taken in a round bottom flask followed by addition of dry acetonitrile. Then the mixture was refluxed at $146\text{ }^\circ\text{C}$ for 16 – 20 h, and the progress of the reaction was monitored by TLC. After maximum consumption of 1-(p-tolyl)ethan-1-one, the solvent was evaporated under reduced pressure, and excess p-Toluenesulfonic acid was neutralised by NaHCO_3 . The organic layer was extracted in DCM, and the crude product was purified through silica gel column chromatography with a solvent gradient system using ethyl acetate and hexane (0–3% EtOAc in hexanes) to obtain the pure product as a white solid (976.42 mg; 75.19% yield). **Characterization of the compound:** ^1H NMR (600 MHz, CDCl_3): δ_{ppm} 7.78 (s, 2H), 7.63–7.65 (d, 4H), 7.32–7.34 (d, 4H), 2.46 (s, 6H), ^{13}C NMR (151 MHz, CDCl_3): δ_{ppm} 142.21, 138.44, 137.30, 129.57, 127.22, 124.61, 21.17; **HRMS (ESI) calcd. for $\text{C}_{27}\text{H}_{24}$ $[\text{M}+\text{H}]^+$:** 349.1951, found: 349.1829.



Scheme S1. Synthesis of 4,4''-dimethyl-5'-(p-tolyl)-1,1':3',1''-terphenyl (compound 1).

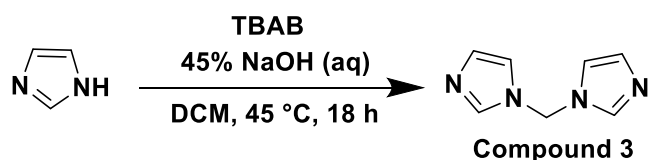
Synthesis of 4,4''-bis(bromomethyl)-5'-(4-(bromomethyl)phenyl)-1,1' (compound 2) — Compound 1 (50 mg, 0.143 mmol, 1 eq.), *N*-Bromosuccinimide (89.38 mg, 0.430 mmol, 3 eq.) and benzoyl peroxide (0.84 mg) were taken in a round bottom flask followed by addition of chloroform. Then the mixture was refluxed at 60 °C for 24 h, and the progress of the reaction was monitored by TLC. After maximum consumption of compound 1, the solvent was evaporated under reduced pressure. The organic layer was extracted in EtOAc, and the crude product was purified through silica gel column chromatography with a solvent gradient system using ethyl acetate and hexane (0 – 5% EtOAc in hexanes) to obtain the pure product as a white solid (976.42 mg; 75.19% yield). **Characterization of the compound:** $^1\text{H NMR}$ (600 MHz, CDCl_3): δ_{ppm} 7.78 (s, 3H), 7.68–7.69 (d, 6H), 7.53–7.54 (d, 6H), 4.60 (s, 6H), $^{13}\text{C NMR}$ (151 MHz, CDCl_3): δ_{ppm} 141.79, 141.06, 137.28, 129.66, 127.76, 125.33, 33.25; **HRMS (ESI) calcd. for $\text{C}_{27}\text{H}_{21}\text{Br}_3$ $[\text{M}+\text{H}]^+$:** 582.9266, found: 582.9065.



Scheme S2. Synthesis of 4,4''-bis(bromomethyl)-5'-(4-(bromomethyl)phenyl)-1,1' (compound 2).

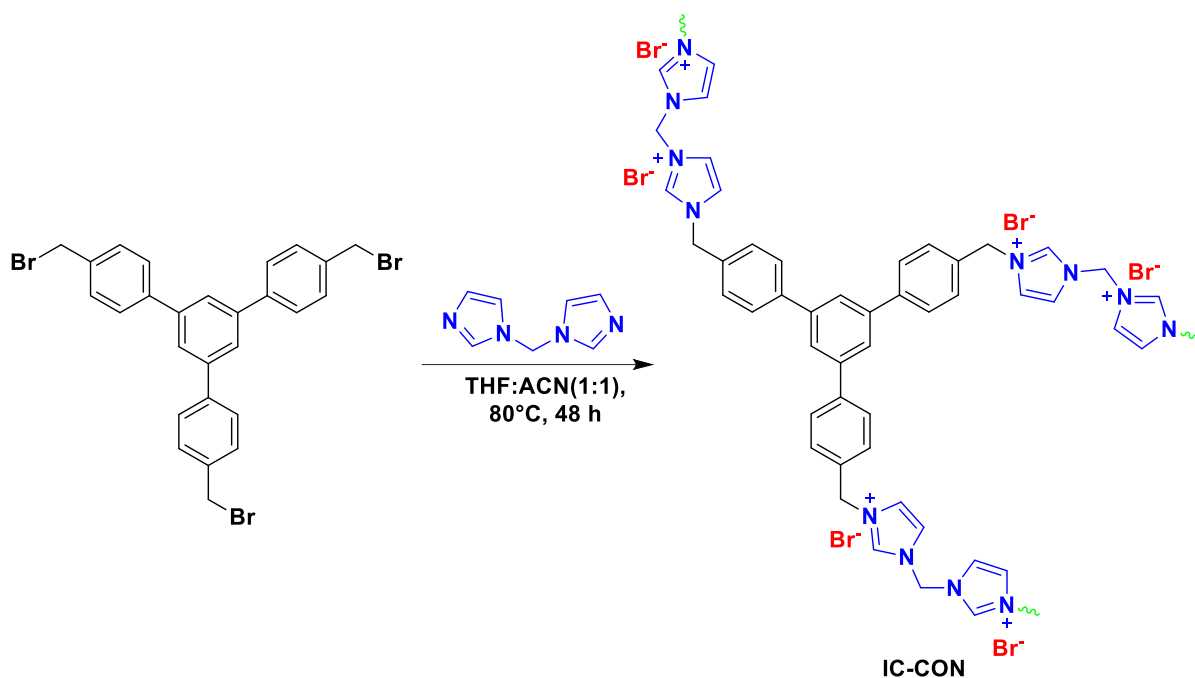
Synthesis of di(1*H*-imidazol-1-yl)methane (compound 3) — A mixture of imidazole (500 mg, 7.34 mmol, 1 eq.) and tetrabutylammonium bromide (47.35 mg, 0.146 mmol, 0.02 eq.) in DCM and 45% NaOH (11 mL) solution was reflux at 45 °C for 16 h, and the progress of the reaction was monitored by TLC. After completion of the reaction, the volatile was removed

from the reaction mixture and the crude product was purified through silica gel column chromatography with a solvent gradient system using MeOH and DCM (0 – 10% MeOH in DCM) to obtain the pure product as a white solid (976.42 mg; 75.19% yield). **Characterization of the compound:** $^1\text{H NMR}$ (600 MHz, CDCl_3): δ_{ppm} 7.93 (s, 2H), 7.39 (s, 2H), 6.91 (d, 2H), 6.22 (s, 2H), $^{13}\text{C NMR}$ (151 MHz, CDCl_3): δ_{ppm} 137.77, 129.58, 119.59, 55.31; **HRMS (ESI) calcd. for $\text{C}_7\text{H}_8\text{N}_4$ $[\text{M}+\text{H}]^+$:** 149.0822, found: 149.0824.



Scheme S3. Synthesis of di(1*H*-imidazol-1-yl)methane (compound 3).

Synthesis of polymer (IC-CON) — Compound 2 and compound 3 were taken in a sealed tube, followed by the addition of 1:1 dry acetonitrile and tetrahydrofuran solvent. Then, the mixture was refluxed at 80 °C for 48 h under inert conditions. After that, the white solid precepted was filtered and washed with various organic solvents, followed by acetonitrile and tetrahydrofuran several times. The compound was dried at 70 °C 24 h and collected. **Characterization of the compound: solid-state FT-IR (cm^{-1}):** 3064 (br), 1600-1500, 1443 (S), 1396 (S), 1350 (S), 1153(S), 1020 (S), 829 (S), 757 (S).



Scheme S4. Synthesis of bis-imidazolium-based cationic covalent organic network (IC-CON).

FT-IR spectroscopy analysis:

The FT-IR spectra of all the samples were recorded using a Perkin Elmer instrument in attenuated total reflectance (ATR) mode over a range of 400–4000 cm^{-1} .

X-ray photoelectron spectroscopy (XPS):

XPS was conducted using a Thermo Fisher Scientific instrument (Serial No.: KAS2020) equipped with an Aluminium $\text{K}\alpha$ source to determine the elemental composition and local bonding environments. The samples were prepared by dispersing the 0.5 mg of the sample in ~ 1 mL milli-Q water, followed by drop-casting it onto a silicon substrate. The samples were dried at room temperature overnight before the analysis.

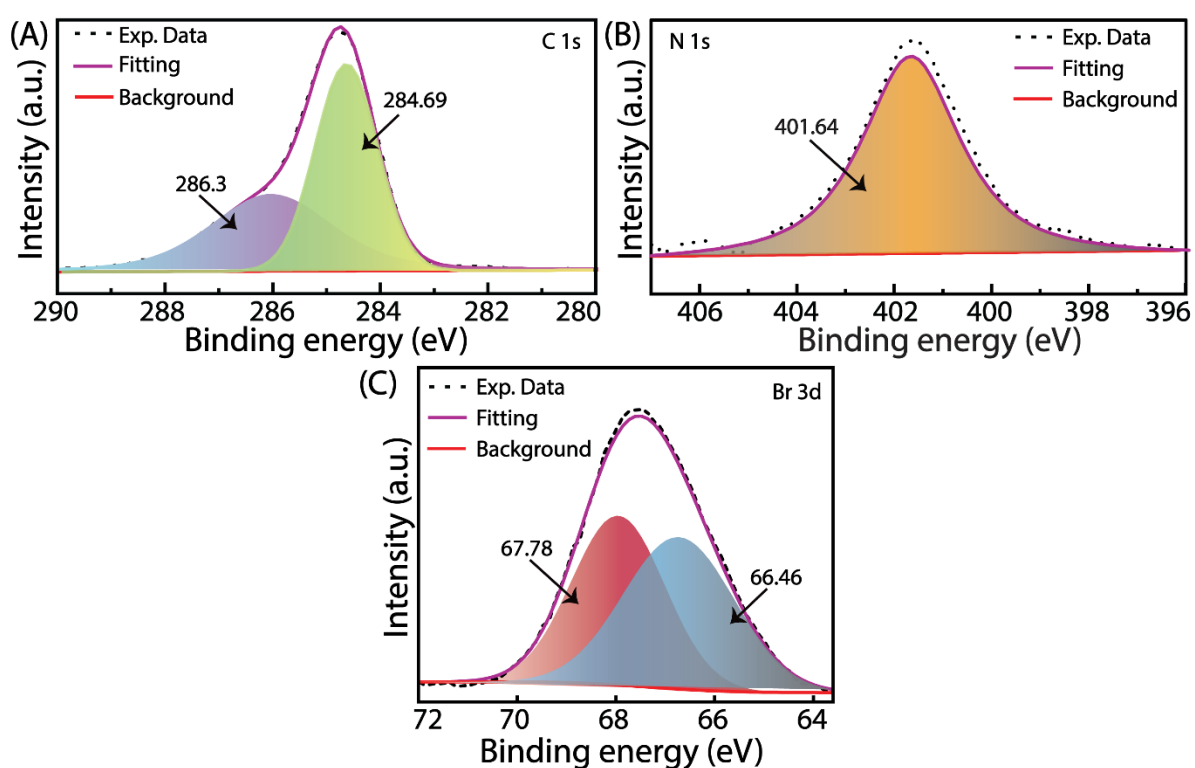


Fig. S1. XPS data profile: the deconvoluted peak of C 1s (A), N 1s (B), and Br 3d of IC-CON.

Powder X-ray Diffraction (PXRD) analysis:

PXRD analysis of the polymer was performed at room temperature using the Phillips PAN analytical diffractometer for Cu K radiation ($= 1.5406$, 40 kV, 40 mA) and the Rigaku MicroMax 007HF diffractometer, respectively.

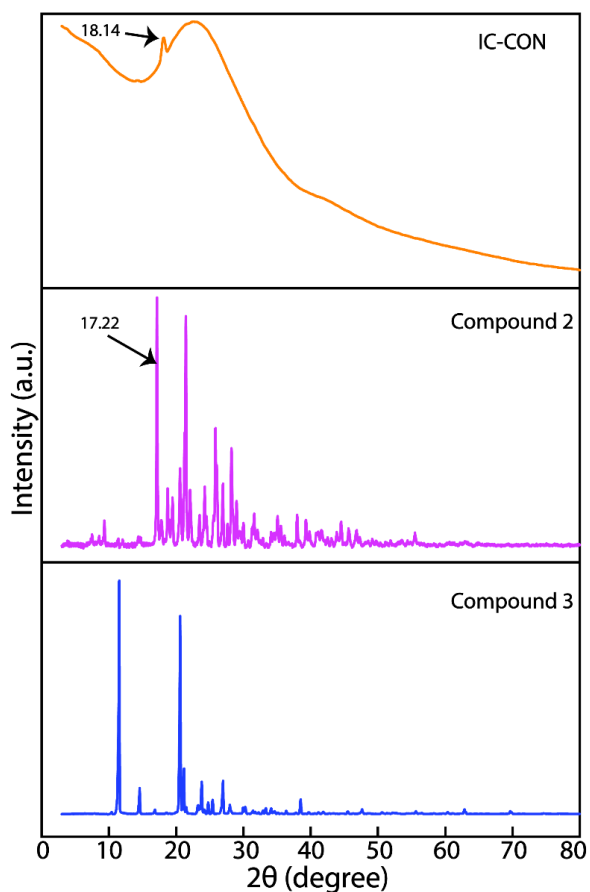


Fig. S2. Comparative PXRD analyses of compounds 2 and 3 with IC-CON.

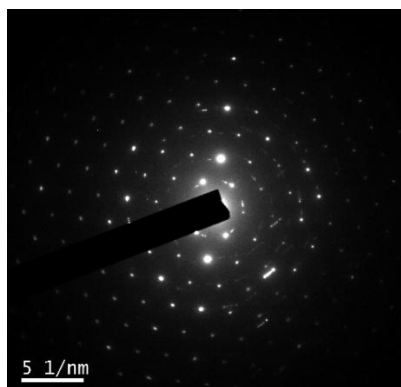


Fig. S3. Transmission electron microscopy -selected area electron diffraction (TEM-SAED) image of IC-CON polymer.

Field emission scanning electron microscopy (FESEM) and FESEM - energy dispersive X-Ray spectroscopy (FESEM-EDX) analysis:

The FESEM analysis was performed using an OXFORD EDS FESEM instrument of the Zeiss Sigma model at 3 kV to determine the morphological analysis of all the tested samples. Similarly, FESEM-EDX analysis was also conducted on the same instrument at 5 kV to analyse

the elemental compositions of all the tested samples. For FESEM and FESEM-EDX analysis, < 0.5 mg of the sample was dispersed in 1 mL of the aqueous solution, followed by drop-casting it onto a silicon substrate. After that, the sample was dried overnight before the analysis was conducted.

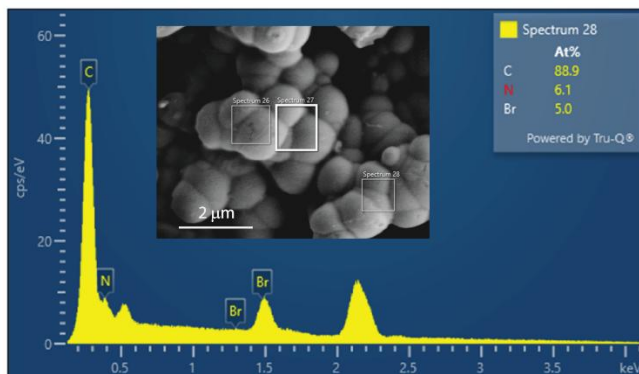


Fig. S4. FESEM-EDX analysis of IC-CON polymer in atomic %.

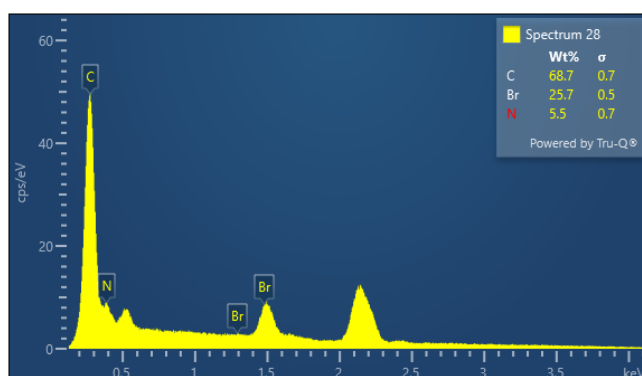


Fig. S5. FESEM-EDX analysis of IC-CON polymer in weight %.

Transmission electron microscopy (TEM):

TEM imaging was performed using JEOL JEM 2100 transmission electron microscope, operating at a maximum accelerating voltage of 200 kV. Samples were prepared for the analysis by dispersing < 0.5mg of the polymer in 5 mL milli-Q water and sonicated for 5 min. Subsequently, 10 μL of the suspension solution was drop-casted onto a carbon-coated copper grid and left for 5 min to settle. Following the gentle blotting of the grid with filter paper, it was allowed to dry overnight at room temperature before analysis.

Atomic force microscopy (AFM):

For AFM analysis, the samples were prepared using the drop-casting technique by dispersing < 0.5 mg of the polymer in 5 mL milli-Q water. Subsequently, 10 μL of the polymer suspension

solutions is deposited onto a silicon wafer and allowed to dry overnight at room temperature. Asylum AFM AC 240 TS-R3 silicon cantilever probes were used to image the samples. Images of the samples were acquired and analysed through standard AC mode imaging, including topographic, amplitude, and phase images.

Thermogravimetric analysis (TGA):

A TGA analysis was performed to assess the thermal stability of the polymer. In this experiment, the polymer sample (10 mg) was heated from 20 °C to 900 °C at a rate of 10 °C min⁻¹ using a Mettler-Toledo TG50 and SDT Q600 TG-DTA analyzer under an N₂ atmosphere.

Nitrogen adsorption Brunauer-Emmett-Teller (BET) experiments:

Quantachrome Quadrasorb automatic and Autosorb IQ instruments were used to conduct the Brunauer-Emmett-Teller (BET) adsorption experiment. Nitrogen adsorption isotherms were measured at 77.3 K, and the temperature was maintained by a liquid nitrogen bath. The samples were activated under vacuum at 150 °C for 4 hours before surface area analysis. The porosity measurement of the activated samples was carried out through the N₂ adsorption technique at 77.3 K, and the average pore diameter measurement was carried out via the Barrett-Joyner-Halenda (BJH) method. The BET surface area of the samples was calculated by multipoint BET analysis, where 'P' and 'P₀' correspond to the equilibrium pressure and saturation pressure of nitrogen in the experimental setup, respectively.

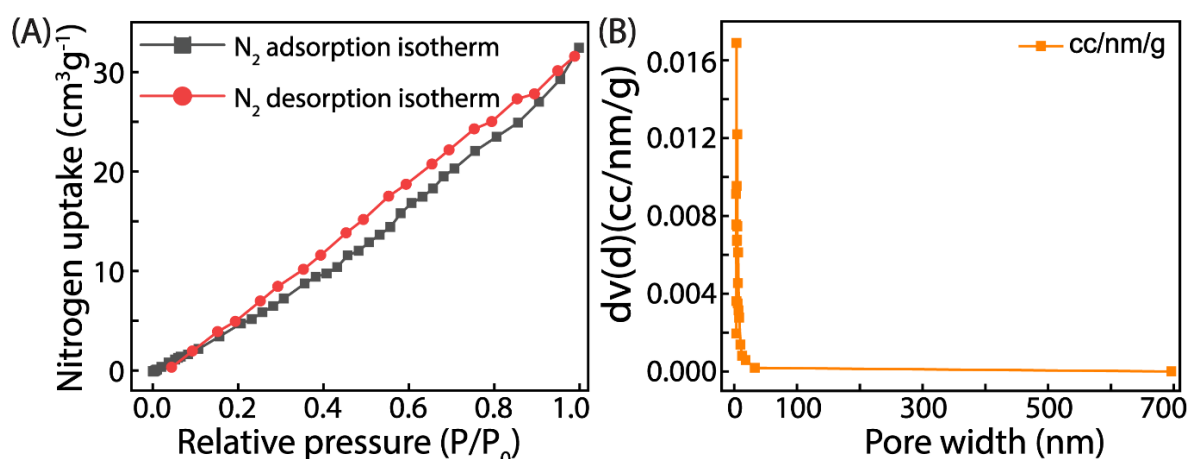


Fig. S6. Nitrogen adsorption isotherm (A) and the pore-size distribution (B) of IC-CON polymer.

Zeta potential study:

To assess the surface charge, zeta potential of the IC-CON was measured at different pH levels ranging from 2 to 12. The pH of the solutions was adjusted using 0.1 M HCl and 0.1 M NaOH. For the analysis, < 0.5 mg of the polymer was dispersed in 1 mL of Milli-Q water at varying pH levels, followed by agitation for 1 minute at room temperature. The surface potential of the samples was then measured at 25 °C using the Zetasizer Nano ZS90 instrument (Malvern, Westborough, MA).

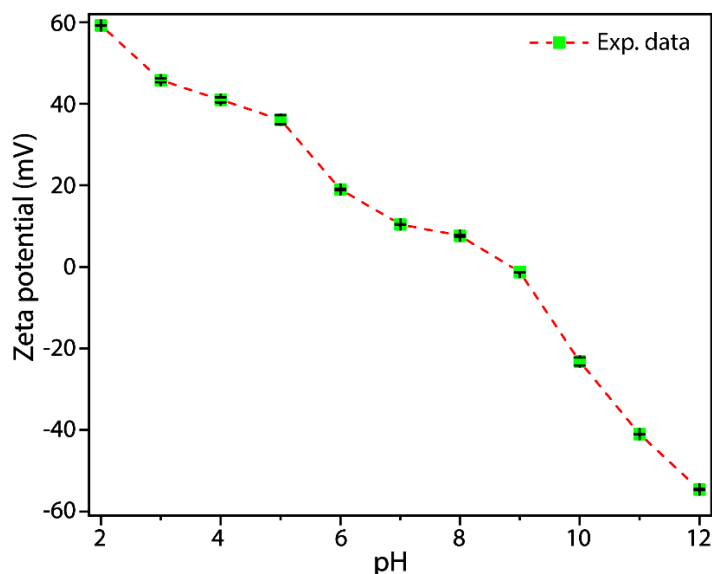


Fig. S7. Zeta potential of IC-CON polymer at different pH.

Tyndall effect:

The Tyndall effect was evaluated by treating ≤ 5 mg of the polymer in Milli-Q water, followed by sonication for 1 minute. Subsequently, a laser light with a wavelength range of 640–660 nm and a maximum output of <1 mW was passed through the polymer solution at different time intervals. A reference solution (blank) of pure deionized water was used as a control.

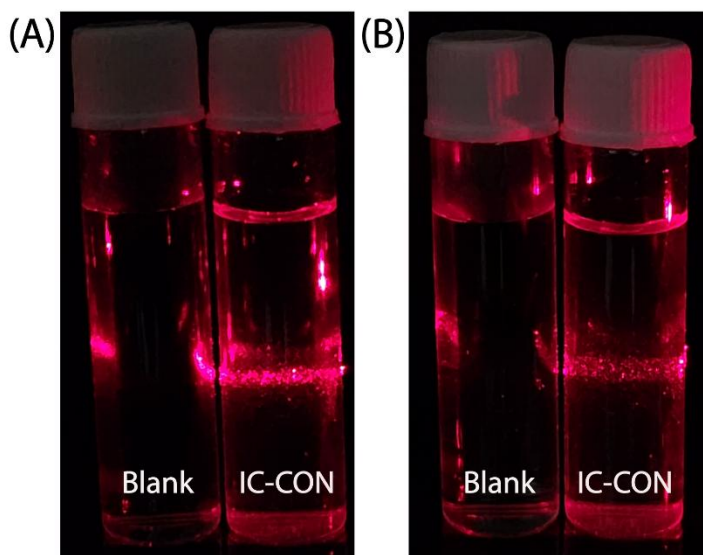


Fig. S8. Tyndall effect of light in the aqueous dispersions of **IC-CON** after 2 min (A) and 48 h (B) of sonication.

Dynamic light scattering (DLS) study of the IC-CON:

DLS and zeta potential analyses were performed using the Zetasizer Nano ZS90 instrument (Malvern, Westborough, MA). For sample preparation, ≤ 0.5 mg of the polymer was dispersed in 1 mL of Milli-Q water and subjected to sonication for 1 minute. The hydrodynamic diameter of the samples was measured at 25 °C at various time intervals (0 h, 6 h, 12 h, 24 h, 36 h, and 48 h).

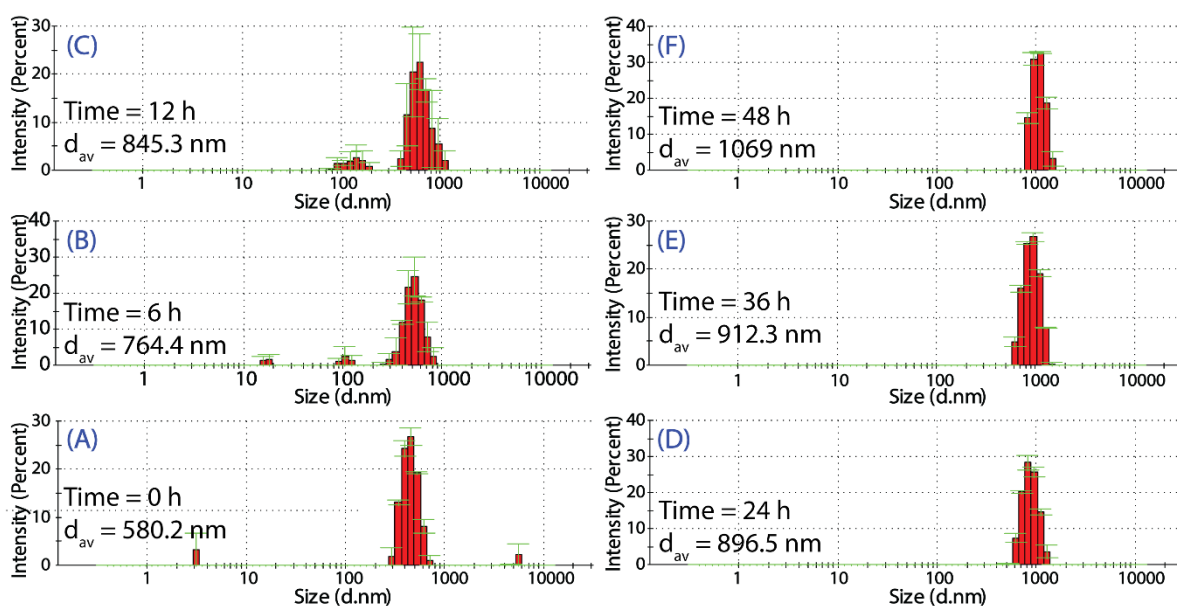


Fig. S9. DLS measurements of **IC-CON** polymer in water at different time intervals.

Chemical stability of the IC-CON:

To access the chemical stability of the IC-CON in different organic solvents, 5 mg of the polymer was separately treated with 5 mL of acetonitrile (ACN), dichloromethane (DCM), ethyl acetate (EtOAc), methanol (MeOH), tetrahydrofuran (THF), and acetone for 21 days. Subsequently, the polymers were isolated from the solvents using centrifugation at 8000 rpm for 5 min, followed by filtration by using a 0.45 μm syringe filter (Axiva). FT-IR analysis was then performed to assess the chemical stability of the polymer after oven drying at 75 $^{\circ}\text{C}$ for 8 h. Additionally, the stability of the IC-CON in basic and acidic solutions was accessed by treating 5 mg of the polymer in 5 mL of HCl (3 N) and NaOH (3 N) for 21 days at room temperature. Following this, the polymers were separated and dried in the same manner as mentioned above, and FT-IR analysis was performed to assess their chemical stability. Furthermore, morphological and thermal stability were assessed using FESEM and TGA on the same IC-CON samples after exposure to the acidic and basic conditions.

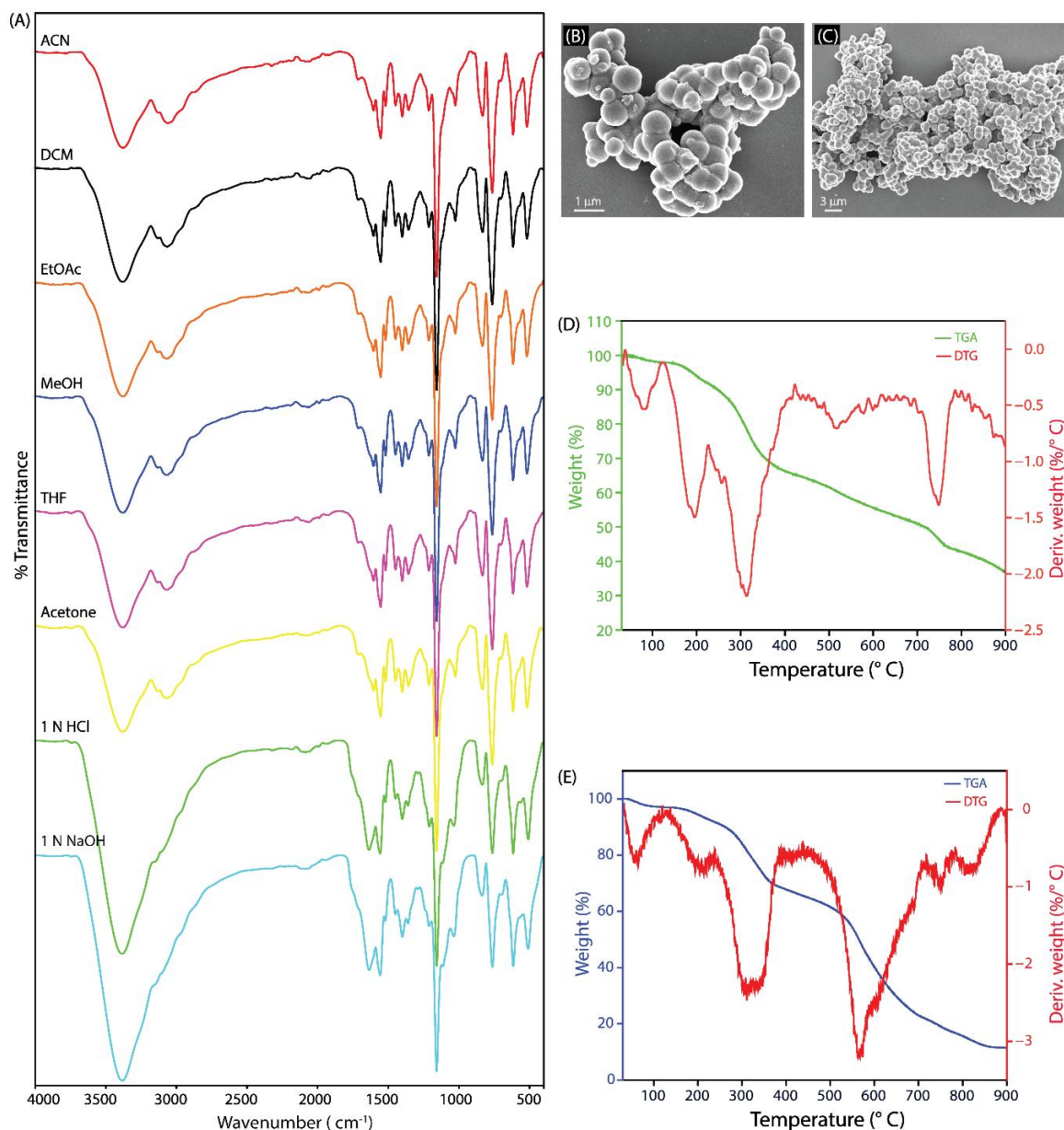


Fig. S10. FT-IR spectra of IC-CON polymer after the treatment (for 21 days) with ACN, DCM, EtOAc, MeOH, THF, DMF, Acetone, HCl (3 N), and NaOH (3 N) solution (A). FESEM images of IC-CON polymer after treatment with 3 N NaOH (A) and 3 N HCl (B) for 21 days. TGA graph of IC-CON polymer after treatment with 3 N NaOH (A) and 3 N HCl (B) for 21 days.

Adsorption study:

Anions adsorption study— All arsenate ion adsorption studies, including selectivity, adsorption isotherm, kinetics, recyclability, and desorption isotherm experiments, were conducted using an Agilent 7850 Inductively Coupled Plasma Mass Spectrometer (ICP-MS). The residual solute concentration in the solution was quantified by comparison with a calibration curve constructed from certified standard solutions of known concentrations. In

contrast, all phosphate ion adsorption experiments were performed using a Metrohm ion chromatograph (792 Basic IC, Switzerland) equipped with a METROSEP A Supp 5-250/4.0 (6.1006.530) separation column (4 mm × 100 mm). The primary standard employed for these measurements was the PRIMUS multi-anion solution (10 mg/kg ± 0.2% for each ionic species) from Fluka. Prior to analysis, arsenate ion solutions were diluted with 2% HNO₃, whereas phosphate ion solutions were diluted using Milli-Q water.

Calculation of % anions adsorption— The relative percentage of the anions adsorption from water has been calculated by using the following equation:

Percentage of adsorption,

$$Q_{ad}(\%) = \frac{(C_0 - C_e)}{C_0} * 100\% \dots \text{Eq. (1)}$$

Where, $Q_{ad}(\%)$ is the relative percentage adsorption, C_0 and C_e are the concentration of anions in ppm (mg/L) before and after treatment of polymers, respectively.

Calculation for equilibrium adsorption capacity— The equilibrium adsorption capacity of the anions by the polymer was calculated by the following Eq. (2).

$$Q_e = \frac{(C_0 - C_e)}{m} V * n \dots \text{Eq. (2)}$$

Where, Q_e = equilibrium adsorption capacity (mg g⁻¹), C_0 = initial concentration (ppm), C_e = equilibrium concentration (ppm), V = volume of solution (mL), m = amount of adsorbent (mg), and n = dilution factor.

Adsorption isotherm equation— Langmuir isotherm (Equation (3)) and Freundlich isotherm models (Equation (4)) were used to fit the adsorption data to find out the maximum adsorption capacity of the anions by the polymer.

$$Q_e = \frac{Q_m K_l C_e}{1 + K_l C_e} \dots \text{Eq. (3)}$$

$$Q_e = K_f C_e^{1/n} \dots \text{Eq. (4)}$$

Where C_e is the equilibrium anion concentration (ppm), Q_e is the corresponding adsorption capacity (mg g⁻¹). The K_l is the Langmuir constant, and Q_m is the max adsorption capacity for the Langmuir model. The K_f and n are the Freundlich constants. For Freundlich adsorption

isotherm, the K_f is associated with the adsorption capacity of the polymer. Whereas $1/n$ describes the extent of adsorption (favourable $1/n < 1$ or unfavourable $1/n > 2$).

Adsorption kinetics equations—The time-dependent adsorption data were fitted in the pseudo-first-order kinetics model and the pseudo-second-order kinetics model, as given in equations (5) and (6), respectively to explore the sorption mechanism.

$$\ln(Q_e - Q_t) = \ln Q_e - k_1 t \dots \text{Eq. (5)}$$

$$\frac{t}{Q_t} = \frac{1}{Q_e^2 k_2} + \frac{t}{Q_e} \dots \text{Eq. (6)}$$

Where Q_t and Q_e (mg g^{-1}) are the adsorption capacities of anion at time t and at equilibrium, respectively. The k_1 and k_2 (g mg sec^{-1}) are the adsorption rate constants of the pseudo-first-order equation and the pseudo-second-order equation, respectively.

Initial binding efficacy study of IC-CON for arsenate and phosphate ions:

This study aimed to evaluate the initial binding efficacy of IC-CON toward arsenate and phosphate ions. The adsorption performance of IC-CON was first assessed for arsenate, followed by an evaluation of its phosphate adsorption capacity upon demonstrating significant arsenate binding efficacy.

For the adsorption experiments, 5 mg of IC-CON was dispersed in 5 mL of a 20-ppm arsenate solution and subjected to sonication for 1 min. The mixture was then agitated at 180 rpm for 5 min using an orbital shaker. Subsequently, the IC-CON was separated from the solution via centrifugation at 8000 rpm for 5 min, followed by filtration through 0.45 μm syringe filters (Axiva). The filtrates containing arsenate were diluted 20-fold to ensure arsenate ion concentrations remained below 1 ppm. The arsenate concentration in the solution before and after IC-CON treatment was quantified.

Encouraged by the high arsenate adsorption efficacy, the phosphate removal capacity of IC-CON was investigated following the same experimental protocol.

Furthermore, the binding efficacy of IC-CON toward arsenate and phosphate was validated using complementary analytical techniques, including Fourier transform infrared spectroscopy (FT-IR), X-ray photoelectron spectroscopy (XPS), field emission scanning electron microscopy coupled with energy dispersive X-ray spectroscopy (FESEM-EDX), and elemental mapping analysis.

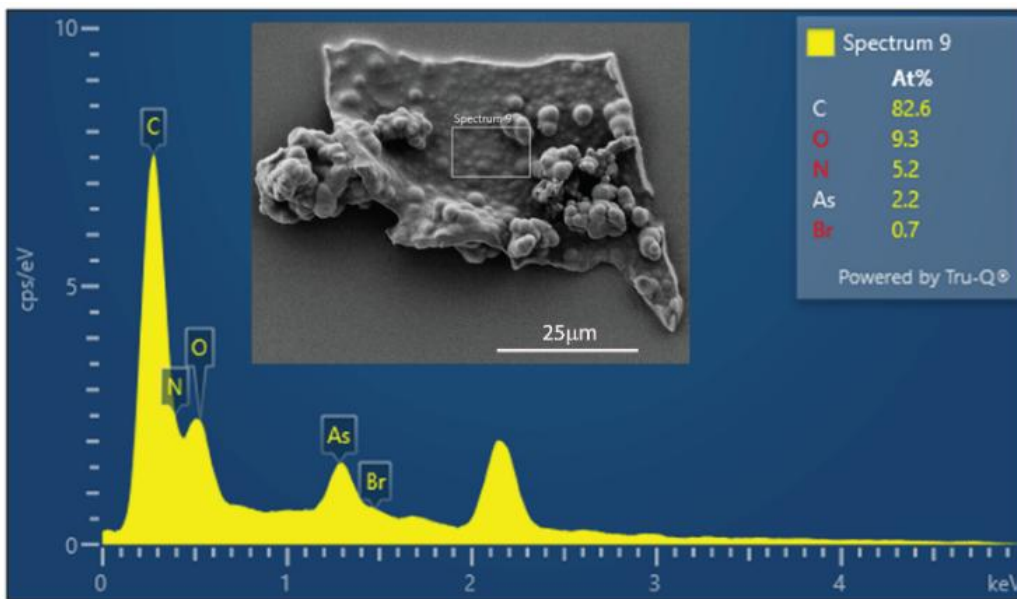


Fig. S11. FESEM-EDX analysis of IC-CON polymer after arsenate adsorption in atomic %.

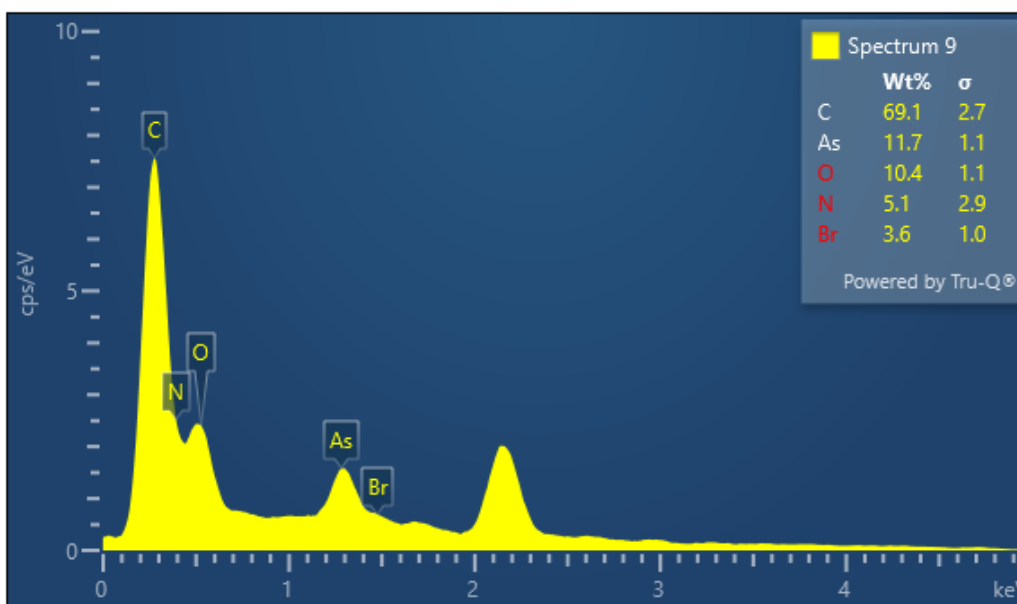


Fig. S12. FESEM-EDX analysis of IC-CON polymer after arsenate adsorption in weight %.

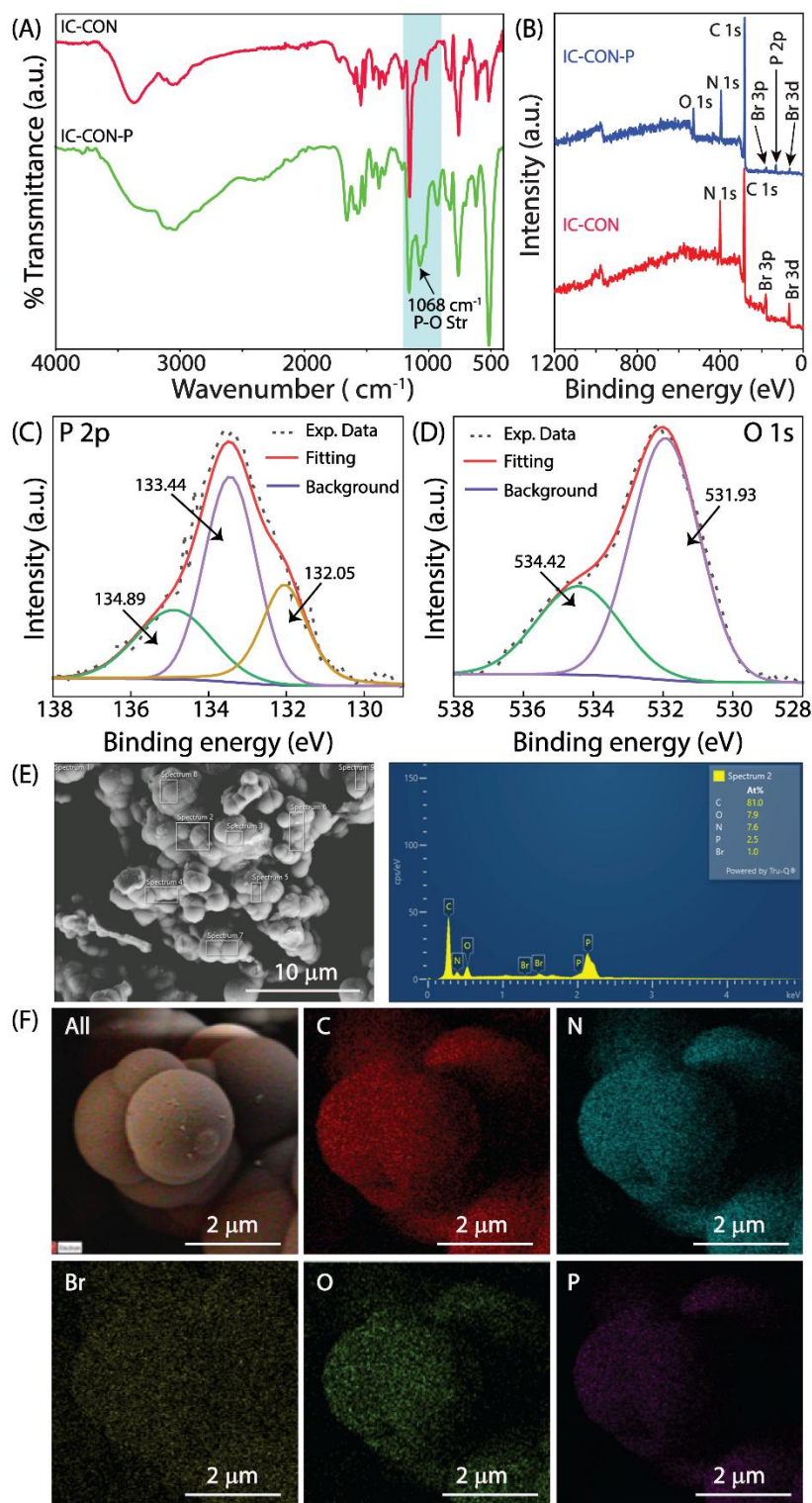


Fig. S13. FT-IR spectra of IC-CON before and after phosphate anion adsorption (A). XPS data profile (wide scan) of IC-CON after phosphate anion adsorption (B). XPS data profile: the deconvoluted peak of P 2p (C), and O1s (D) of IC-CON polymer after phosphate adsorption. FESEM-EDX analysis of IC-CON polymer after phosphate adsorption in atomic % (E). The FESEM mapping analysis for the C, O, N, Br and P of IC-CON after phosphate anion adsorption (F).

Influence of pH on adsorption experiments:

To evaluate the effect of pH on the adsorption of arsenate and phosphate ions by IC-CON, adsorption experiments were conducted over a pH range of 2 to 12. The pH of the solutions was adjusted using 0.1 M HCl and 0.1 M NaOH. In each experiment, 5 mg of the polymer was added to 5 mL of a 500-ppm arsenate ion solution prepared at different pH values (2, 4, 5, 6, 7, 8, 10, and 12) and agitated in an orbital shaker at 180 rpm for 6 hours at 25 °C. Following adsorption, the polymer was separated from the solution via centrifugation at 8000 rpm for 5 minutes, followed by filtration using a 0.45 μm syringe filter (Axiva). The residual arsenate ion concentration in the supernatant was determined using ICP-MS. Prior to analysis, the supernatants were diluted 500 times to maintain arsenate ion concentrations below 1 ppm. The equilibrium adsorption capacity of the polymer for arsenate ions was subsequently calculated using Equation 2.

Similarly, the effect of pH on phosphate ion adsorption was investigated following the same procedure. In this case, IC was employed to quantify the phosphate ion concentration in the supernatants before and after treatment with IC-CON. To ensure phosphate ion concentrations remained below 20 ppm, each solution was diluted 25 times before IC analysis.

The results of the above analyses reveal that both the arsenate and phosphate ion adsorption capacities reach their maximum values under near-neutral conditions (pH 6–8). The adsorption of arsenate and phosphate ions by IC-CON is predominantly influenced by two non-covalent interactions: hydrogen bonding with the acidic C–H protons near the quaternary nitrogen centres and electrostatic attraction between the quaternary nitrogen and the anionic species. The zeta potential study revealed that the surface potential of IC-CON increases from +7 mV at pH 7 to +45 mV at pH 2, signifying a higher positively charged surface in acidic environments. Despite the increased positive surface charge at lower pH, the adsorption efficacy of both arsenate and phosphate ions decreases. This decrease can be ascribed to two key factors. Initially, the elevated concentration of chloride ions (Cl^-) in acidic conditions competes with arsenate and phosphate for electrostatic binding sites on IC-CON, diminishing their adsorption; additionally, the increased protonation of arsenate and phosphate ions at low pH reduces their net negative charge, thereby weakening electrostatic interactions with the cationic IC-CON surface. As pH rises from 7 to 12, arsenate and phosphate ions undergo gradual deprotonation, resulting in an increase in their negative charge. At alkaline pH, IC-CON exhibits a negative zeta potential, resulting in electrostatic repulsion between the polymer and the anions and hence reducing adsorption. Moreover, the higher concentration of hydroxide ions (OH^-) at high pH competes with arsenate and phosphate for binding sites. Furthermore,

the deprotonation of the oxyanions at elevated pH diminishes their hydrogen-bonding ability, hence further reducing interaction with the IC-CON framework. At pH 7, IC-CON exhibits a moderately positive zeta potential ($\sim +7$ mV), signifying the presence of quaternary ammonium groups that can participate in electrostatic interactions with arsenate and phosphate ions. At this pH, arsenate predominantly exists as H_2AsO_4^- and HAsO_4^{2-} , while phosphate also exists as H_2PO_4^- and HPO_4^{2-} species, which possess hydroxyl functionalities that can engage in directional hydrogen bonding with the electron-deficient $-\text{C}-\text{H}$ protons adjacent to the quaternary nitrogen atoms on the imidazolium rings, thus improving overall adsorption efficacy. Furthermore, the negligible concentration of competing anions such as Cl^- or OH^- at neutral pH helps IC-CON to selectively interact with target arsenate and phosphate ions. This diminished ionic competition, along with synergistic hydrogen bonding and electrostatic attraction, enhances both enthalpic and entropic factors in the adsorption process. Most natural groundwater sources have a pH between 5 and 8, and IC-CON demonstrated enhanced adsorption capacity under near-neutral conditions (pH 6–8), indicating its potential for practical application in diverse water treatment processes.¹

Adsorption isotherms:

To evaluate the adsorption isotherms of arsenate and phosphate ions by the polymer, aqueous solutions of arsenate and phosphate ions were prepared at varying concentrations ranging from 1 to 1200 ppm in Milli-Q water. 5 mL of each solution was individually treated with 5 mg of the IC-CON, followed by sonication for 1 minute to ensure homogeneous dispersion. The samples were then incubated under continuous shaking at 180 rpm in an orbital shaker at room temperature for 6 hours. After incubation, the polymer was separated from the solution via centrifugation at 8000 rpm for 5 minutes, followed by filtration using 0.45 μm syringe filters (Axiva). The filtered supernatants containing arsenate were diluted to maintain arsenate ion concentrations below 1 ppm, while the phosphate-containing supernatants were diluted to maintain phosphate ion concentrations below 20 ppm prior to analysis. The equilibrium concentrations of arsenate and phosphate ions were then determined using Equation 2. To further analyse the adsorption behaviour, both the Langmuir and Freundlich isotherm models, as described in Equations 3 and 4, respectively, were employed to assess the relationship between adsorption parameters and equilibrium concentrations. These models were also used to determine the maximum adsorption capacity of the polymer for arsenate and phosphate ions.

Kinetics study:

The adsorption kinetics of arsenate and phosphate ions onto the polymer were evaluated by monitoring their uptake from aqueous solutions over various time intervals: 15, 30, 45, 60, 90, 120, 150, 180, 210, 240, 270, 300, 360 and 400 seconds. In each experiment, 5 mg of IC-CON was incubated with 5 mL of a 500-ppm aqueous solution of arsenate or phosphate at pH 7. At each designated time point, approximately 100 μ L of the solution was collected, and the polymer was separated via centrifugation at 8000 rpm for 5 minutes, followed by filtration through 0.45 μ m syringe filters (Axiva). The filtered supernatants containing arsenate ions were diluted 500 times to maintain concentrations below 1 ppm before analysis via ICP-MS. Similarly, the filtered phosphate-containing supernatants were diluted 25 times to maintain phosphate ion concentrations below 20 ppm before analysis using IC. The equilibrium concentrations of arsenate and phosphate ions were then calculated using Equation 2. The adsorption kinetics of arsenate and phosphate ions onto the polymer were further characterized by fitting the experimental data to both pseudo-first-order and pseudo-second-order kinetic models, as described by Equations 5 and 6, respectively.

Additionally, to investigate the effect of polymer concentration on adsorption kinetics, experiments were conducted using varying amounts of IC-CON (3 mg, 5 mg, 7 mg, and 10 mg), each incubated with 5 mL of a 500-ppm aqueous solution of arsenate or phosphate at pH 7. The kinetics study for each polymer concentration was performed following the same protocol as described above.

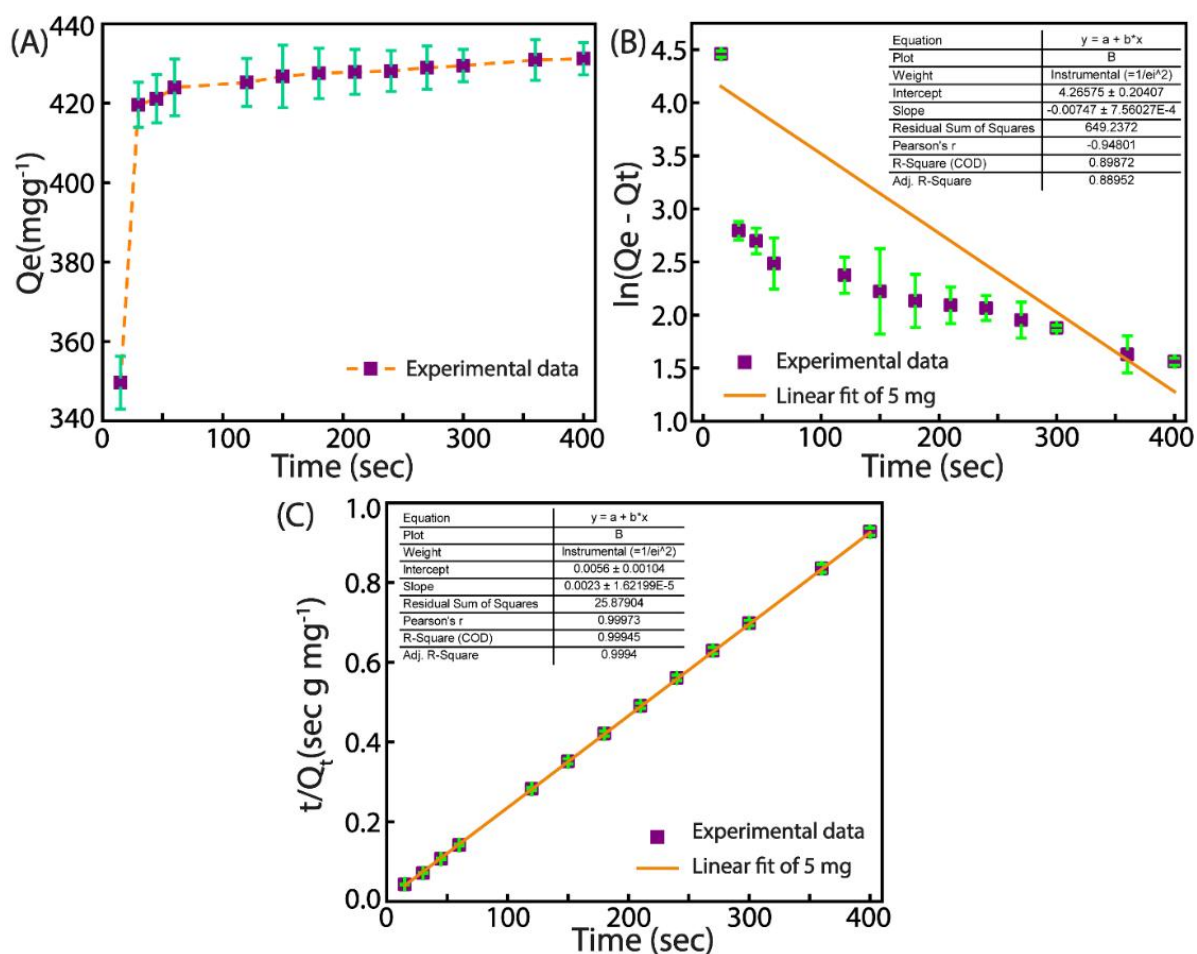


Fig. S14. Time-dependent adsorption isotherm of arsenate by IC-CON (5 mg) at pH 7 under room temperature(A), the time-dependent arsenate adsorption efficiency of IC-CON fitted with the first order (B) and second order kinetics (C) models.

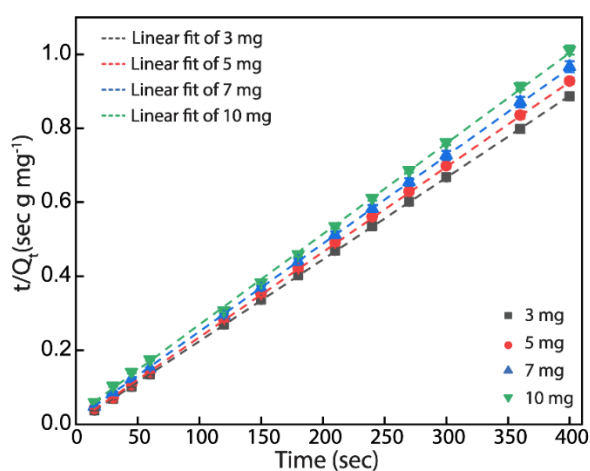


Fig. S15. Pseudo-second-order kinetics curves of arsenate adsorption on IC-CON (3-10 mg) at pH 7.0 under room temperature.

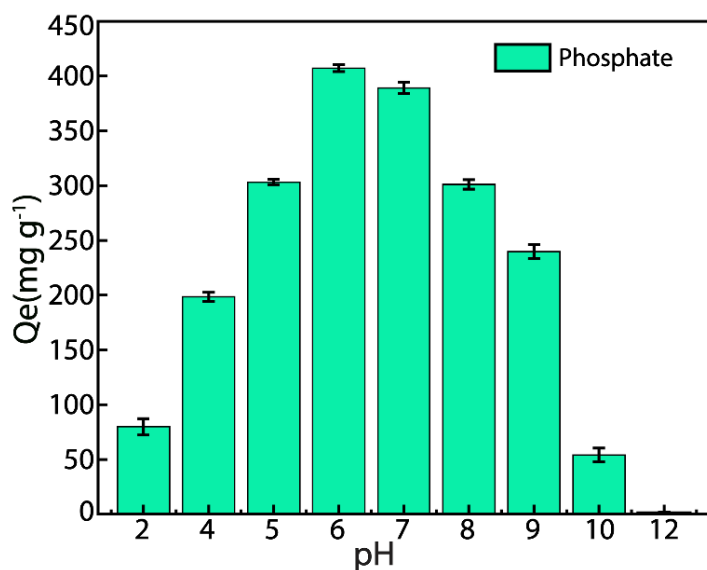


Fig. S16. The pH-dependent phosphate ion adsorption efficiency of IC-CON.

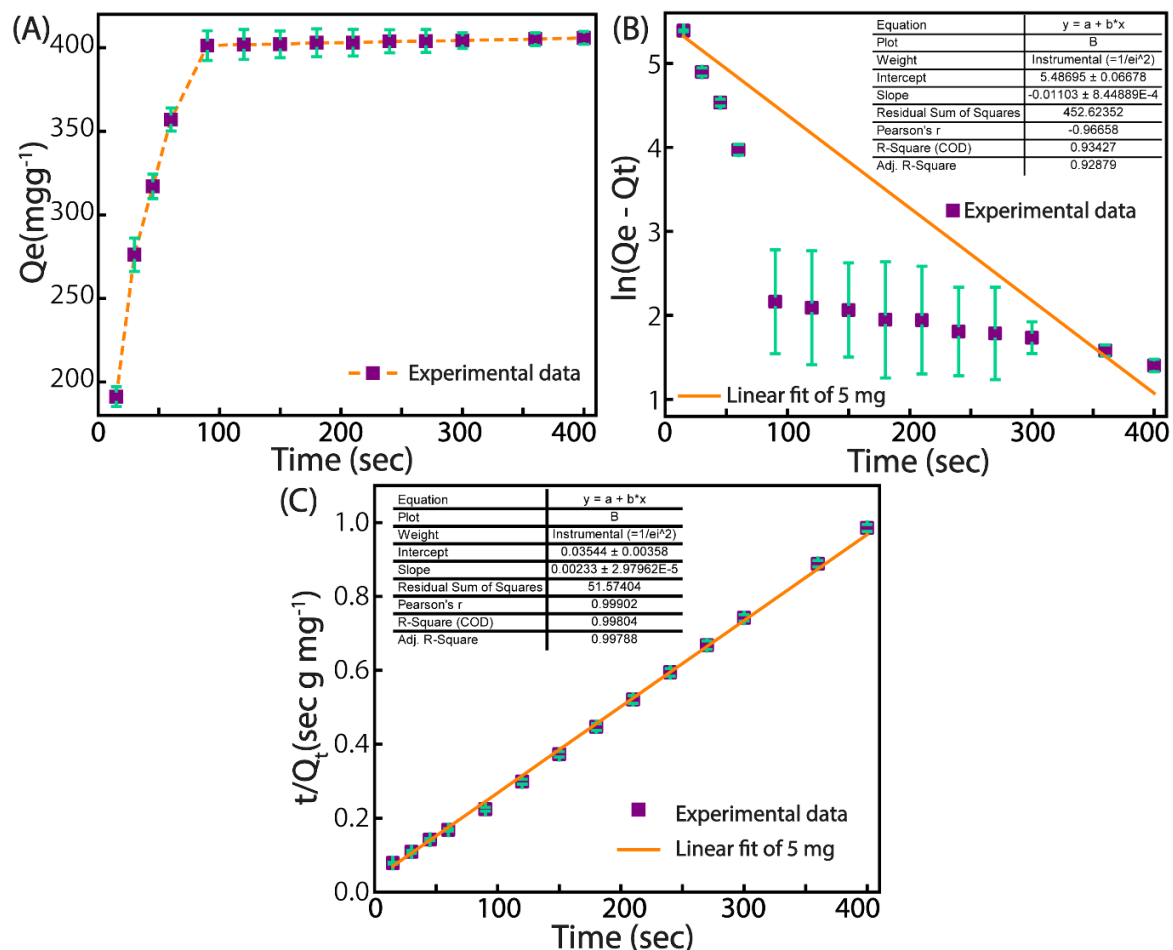


Fig. S17. Time-dependent adsorption isotherm of phosphate by IC-CON (5 mg) at pH 7 under room temperature(A), time-dependent phosphate adsorption efficiency of IC-CON fitted with the first order (B) and second order kinetics (C) models.

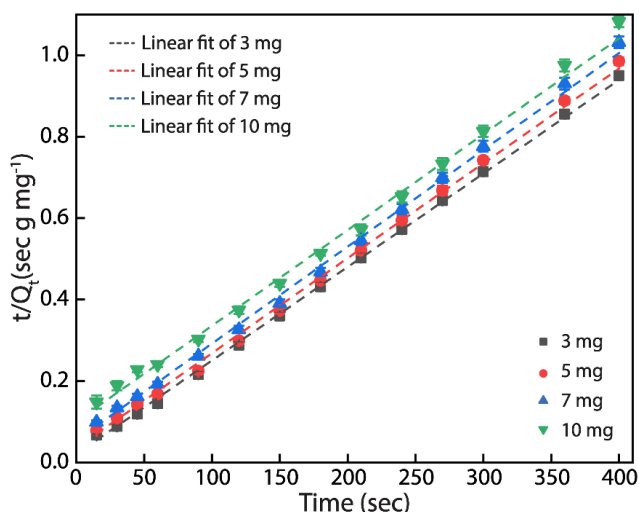


Fig. S18. Pseudo-second-order kinetics curves of phosphate adsorption on IC-CON (3-10 mg) at pH 7.0 under room temperature.

Effect of temperature on phosphate adsorption:

To examine the effect of temperature on arsenate adsorption, four batches of 5 mL arsenate solution (500 ppm) were individually mixed with 5 mg of the IC-CON polymer and agitated for 3 hours at different temperatures (298 K, 313 K, 328 K, and 343 K) at pH 7. Following adsorption, the polymer was separated via centrifugation, and the arsenate concentration in the solution before and after treatment with IC-CON was quantified using ICP-MS. A similar investigation was conducted for phosphate ions, with their concentrations measured before and after adsorption using IC.

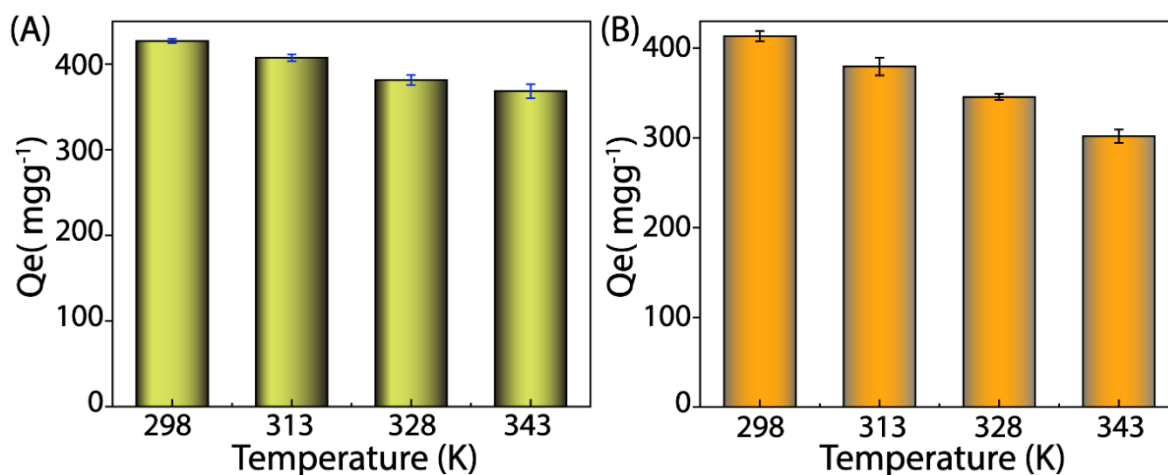


Fig. S19. The equilibrium adsorption capacity of arsenate (A) and phosphate (B) by IC-CON at different temperatures.

Effect of counter anions on phosphate adsorption:

To investigate the influence of competing anions, including Cl^- , F^- , NO_3^- , SO_4^{2-} , and CO_3^{2-} , on the adsorption of arsenate and phosphate, binary stock solutions were prepared using sodium salts of the aforementioned anions in Milli-Q water. These solutions were formulated at varying molar ratios of arsenate or phosphate to competing anions (1:1, 1:10, 1:50, and 1:100) to systematically evaluate their impact on adsorption efficiency. The concentrations of arsenate and phosphate ions in the stock solution were set at 20 ppm, while the concentrations of other ions were adjusted relative to these ions.

Subsequently, 5 mg of the IC-CON polymer was introduced into 5 mL of each stock solution and agitated for 3 hours. The adsorption efficacy of IC-CON for arsenate and phosphate in the presence of competing anions was then assessed.

The results indicate that Cl^- ions exert a negligible influence on the adsorption of arsenate and phosphate by the IC-CON polymer. Consequently, to evaluate the effect of metal cations on arsenate and phosphate adsorption, stock solutions were prepared using different chloride salts following the previously described procedure. Due to the solubility constraints of various metal arsenates and phosphates, metal chloride salts of Na^+ , K^+ , Rb^+ , Cs^+ , Mg^{2+} , and Al^{3+} were selectively employed for this investigation. These experiments were conducted following the same protocol as outlined above.

Two binary stock solutions were prepared to evaluate the adsorption efficacy of IC-CON towards arsenate (As) in the presence of chromate (Cr) and rhenate (Re). One stock solution contained a mixture of 20 ppm arsenate and chromate ions (Sodium chromate), while the other consisted of 20 ppm arsenate and rhenate ions (sodium perrhenate). A 5 mg portion of IC-CON was treated with 5 mL of each stock solution separately and agitated for 6 h at 180 rpm in an orbital shaker under ambient conditions. Following incubation, the polymer was separated from the solution via centrifugation at 8000 rpm for 5 minutes, followed by filtration using 0.45 μm syringe filters (Axiva). The filtered supernatants were subsequently diluted 20-fold to ensure arsenate ion concentrations remained below 1 ppm. The relative removal percentage of arsenate ions was then calculated using Equation 1.

A similar experimental procedure was employed to assess the adsorption capacity of IC-CON for phosphate (P) in the presence of chromate and rhenate ions.

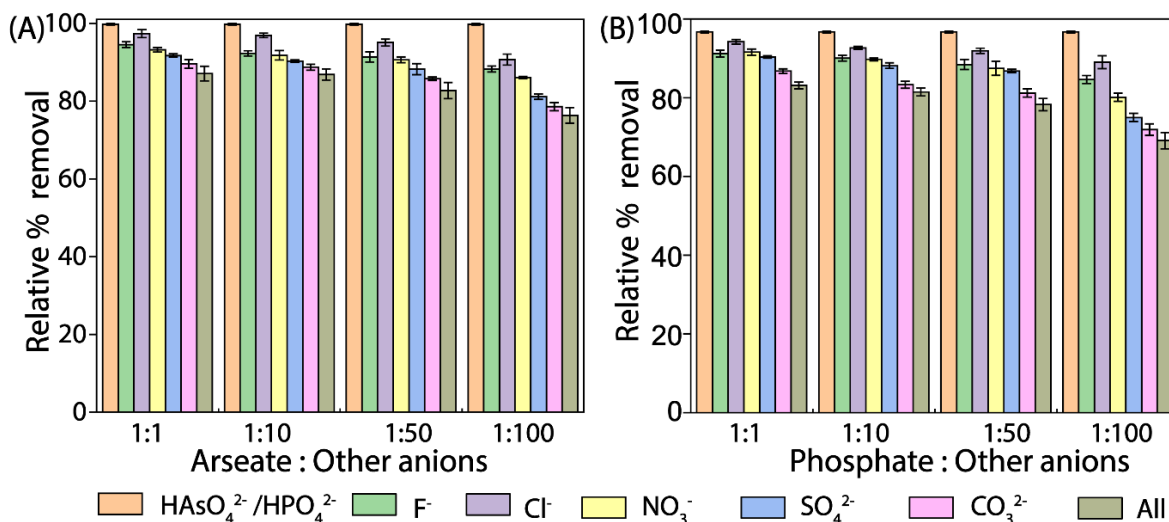


Fig. S20. Arsenate (A) and phosphate (B) removal efficiency of IC-CON polymer in the presence of different ratios of Cl⁻, F⁻, NO₃⁻, SO₄²⁻, and CO₃²⁻ anions.

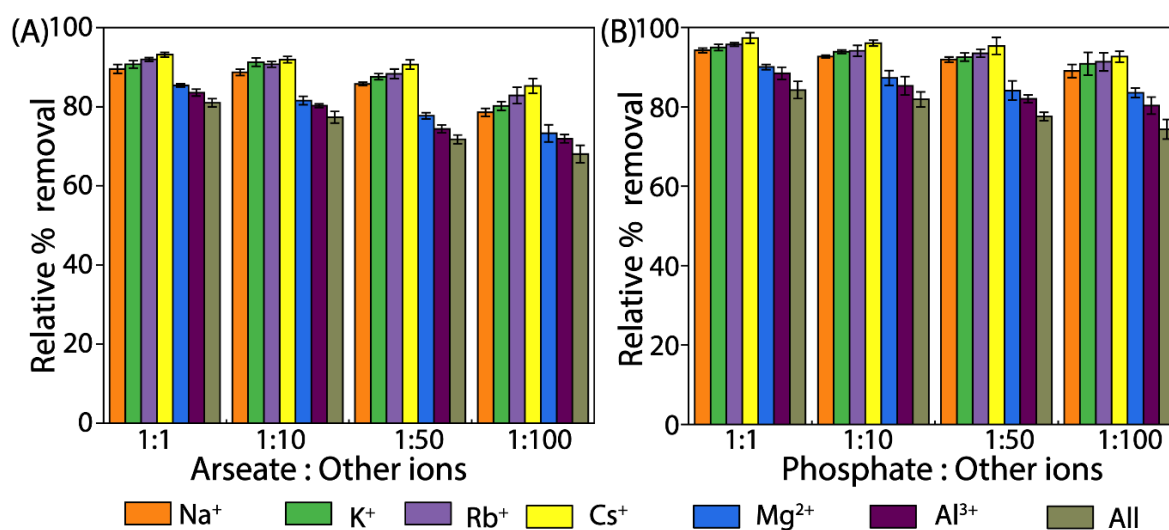


Fig. S21. Arsenate (A) and phosphate (B) removal efficiency of IC-CON polymer in the presence of different ratios of Na⁺, K⁺, Rb⁺, Cs⁺, Mg²⁺, and Al³⁺ ions.

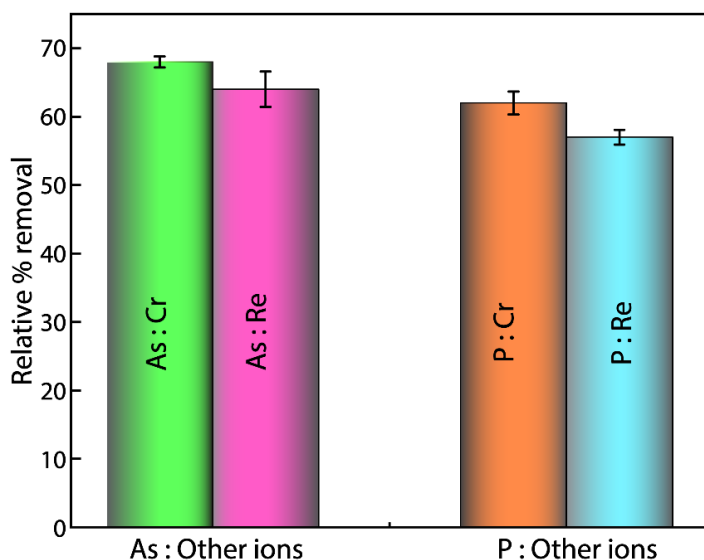


Fig. S22. Arsenate (As) and phosphate (P) removal efficiency of IC-CON polymer in the presence of Cr and Re ions.

Adsorption performance of IC-CON for arsenate and phosphate from equimolar binary solutions at varying concentrations:

To evaluate the selective adsorption efficacy of IC-CON for arsenate and phosphate ions from a 1:1 arsenate-to-phosphate binary solution, five stock solutions with equimolar arsenate and phosphate concentrations ranging from 0.5 ppm to 100 ppm were prepared. Subsequently, 5 mg of the IC-CON polymer was introduced into 5 mL of each stock solution and subjected to agitation for 3 hours. Following adsorption, the polymer was separated via centrifugation, and the residual concentrations of arsenate and phosphate ions in the supernatant were quantified to assess the adsorption performance of IC-CON.

Regeneration analyses of IC-CON:

The reusability of the polymer was systematically assessed through a series of batch experiments involving cyclic adsorption and desorption of phosphate and arsenate ions. In each adsorption cycle, 5 mg of IC-CON was incubated individually with 5 mL of a 500-ppm aqueous solution containing arsenate and phosphate ions. The mixture was subjected to orbital shaking at 180 rpm for 1 hour at room temperature to facilitate adsorption. Subsequently, the polymer was separated from the solution through centrifugation and filtration, effectively isolating the adsorbent loaded with arsenate and/or phosphate ions. The unadsorbed arsenate and phosphate ion concentrations in the supernatant were then quantified.

Desorption of the adsorbed arsenate and phosphate ions was conducted by immersing the loaded IC-CON in 5 mL of a 0.5 N NaOH solution (pH ~13) at room temperature for 2 hours. The desorbed solution was collected and analysed to determine the amount of arsenate and phosphate ions released from the polymer. Following desorption, the IC-CON polymer was subjected to a regeneration process involving thorough washing with a 0.1 N NaBr solution to convert the polymer from the OH⁻ form to the Br⁻ form. Subsequently, extensive rinsing with Milli-Q water was performed to eliminate residual contaminants and restore the adsorption capacity of the polymer. The polymer was then recovered via centrifugation and filtration, followed by drying in a microwave oven at 70 °C for 6 hours before the next adsorption cycle. This adsorption-desorption process was repeated for 15 consecutive cycles, with each adsorption cycle utilizing a fresh 500 ppm stock solution of arsenate and phosphate ions to evaluate the long-term reusability of the polymer.

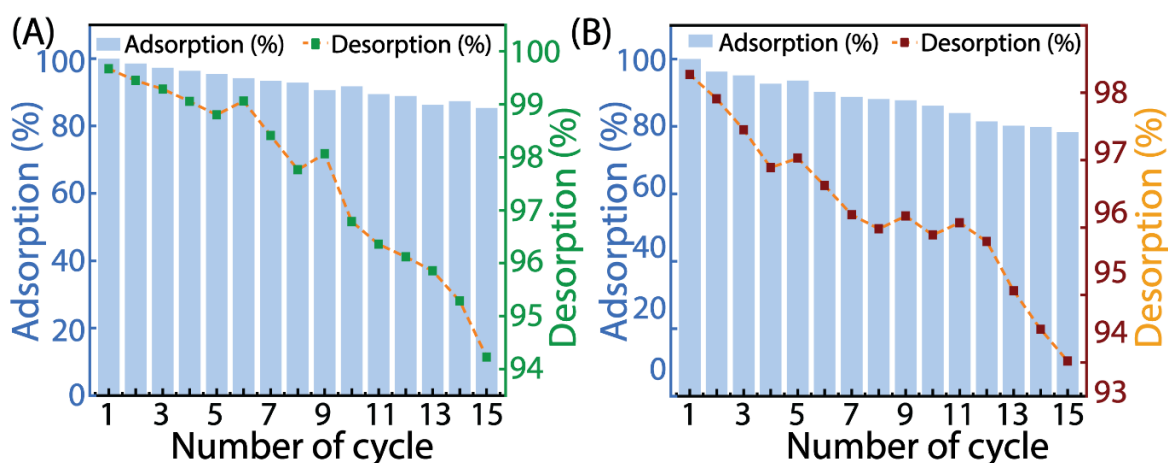


Fig. S23. Arsenate (A) and Phosphate (B) ion adsorption and desorption efficiency of IC-CON after different cycles.

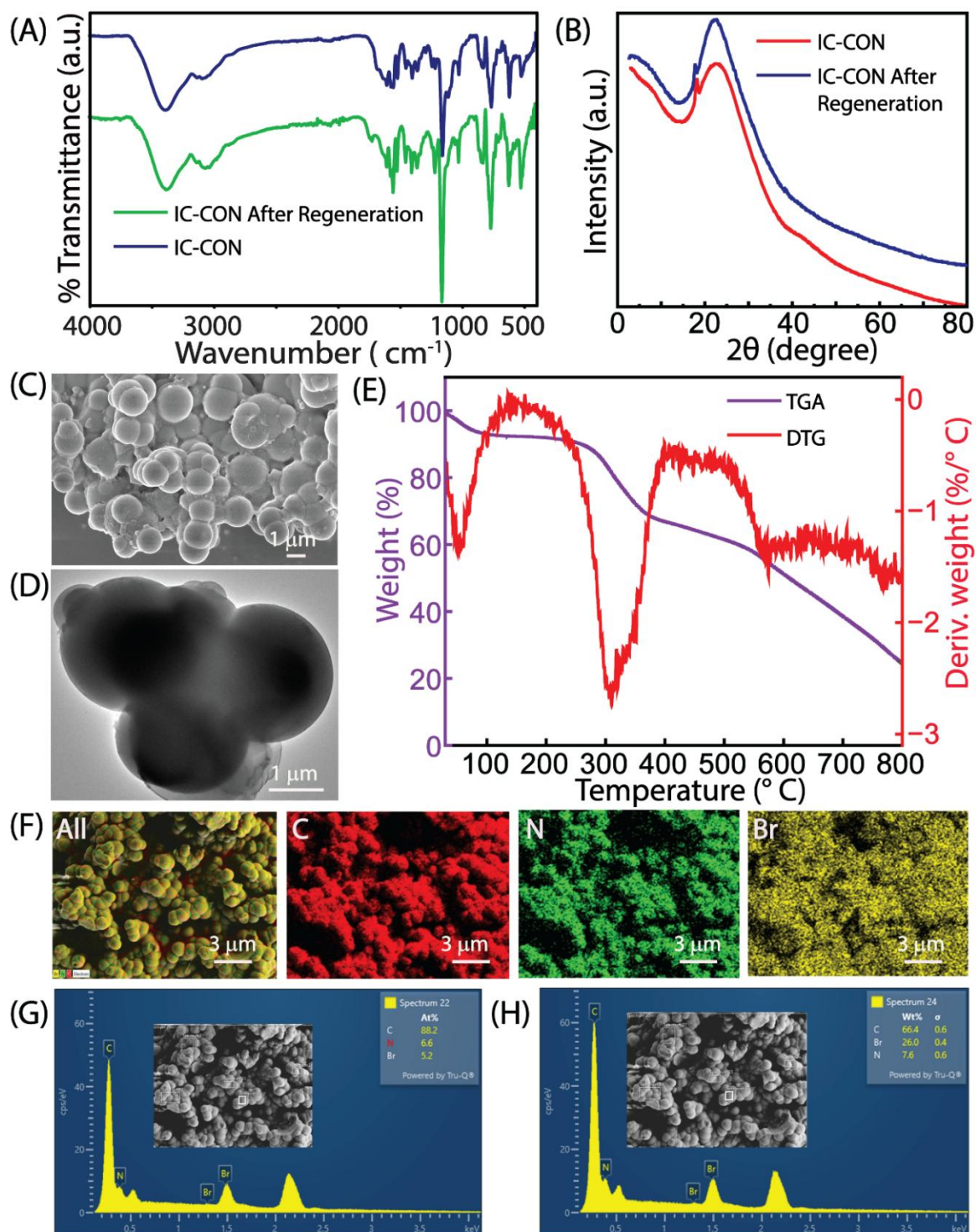


Fig. S24. FT-IR (A), PXRD (B), FESEM image (C), TEM image (D), TGA-DTG analysis (E), FESEM mapping (F) and elemental analysis in atomic % (G) and weight % (H) of **IC-CON** polymer after undergoing 15 cycles of adsorption and desorption of arsenate.

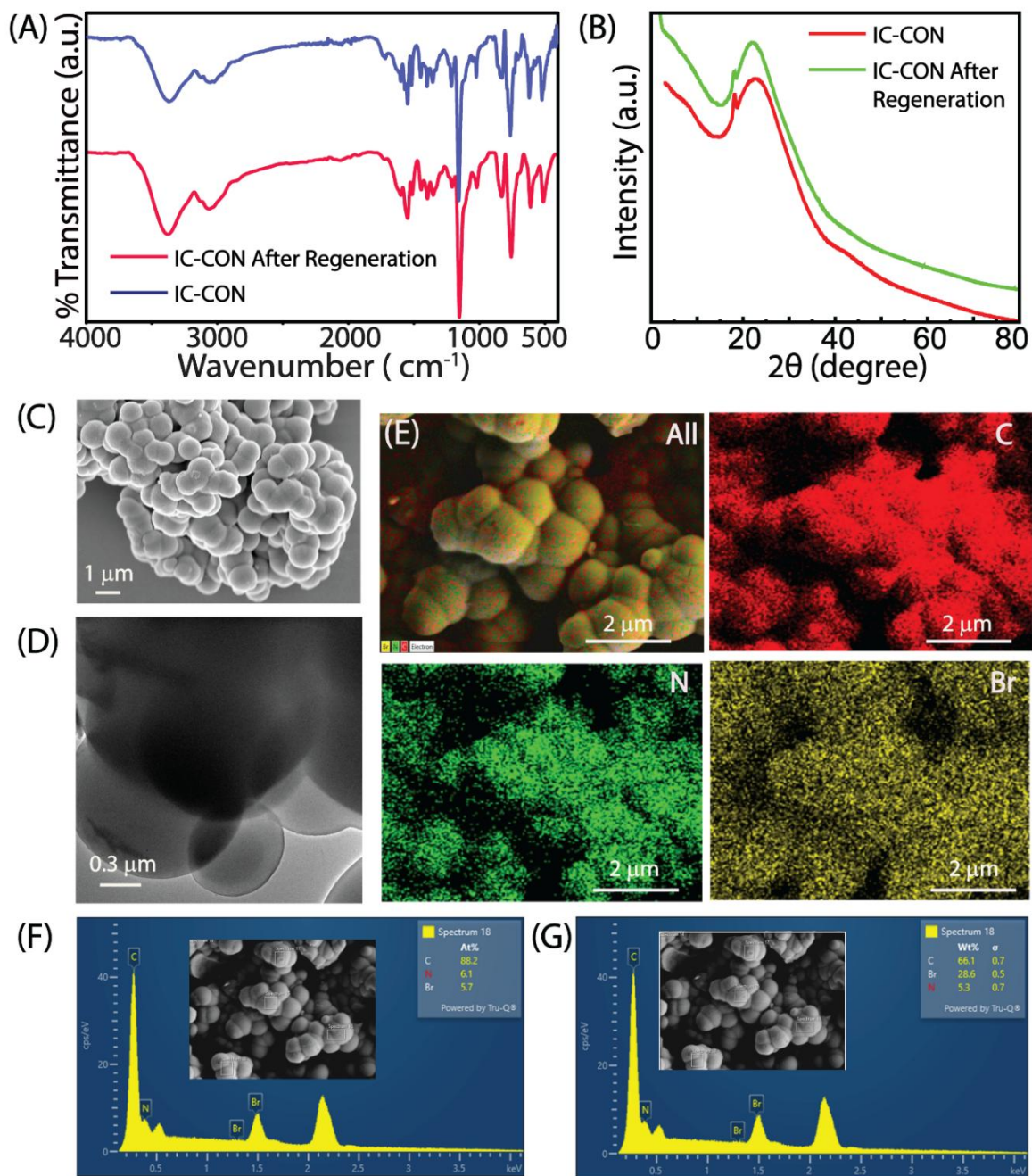


Fig. S25. FT-IR (A), PXRD (B), FESEM image (C), TEM image (D), FESEM mapping (E) and elemental analysis in atomic % (G) and weight % (H) of IC-CON polymer after undergoing 15 cycles of adsorption and desorption of phosphate.

Arsenate and phosphate desorption kinetics — To investigate the desorption kinetics of arsenate and phosphate from the IC-CON polymer, 5 mg of arsenate- and phosphate-loaded polymers were individually mixed with 5 mL of 0.5 N NaOH solution. The suspensions were subjected to continuous agitation using an orbital shaker incubator (LabTech) set at 180 rpm

and maintained at 25°C. At predetermined time intervals (ranging from 2 to 60 min), aliquots were collected, and the polymer was separated via centrifugation followed by filtration. The filtrate containing arsenate was subsequently diluted by a factor of 500 to ensure an arsenate concentration of ≤ 1 ppm, followed by quantification using ICP-MS. Similarly, the filtrate containing phosphate was diluted by a factor of 25 to maintain a phosphate concentration of ≤ 20 ppm, with subsequent analysis conducted using IC. The desorption kinetic data were analysed by plotting them using the linear forms of the pseudo-first-order and pseudo-second-order models. The results confirmed that both desorption processes followed the pseudo-second-order model. Arsenate desorption exhibited a rate constant of $0.000634 \text{ mg g}^{-1} \text{ min}^{-1}$ with a correlation coefficient (R^2) of 0.988, while phosphate desorption showed a rate constant of $0.000172 \text{ mg g}^{-1} \text{ min}^{-1}$ with an R^2 of 0.947.

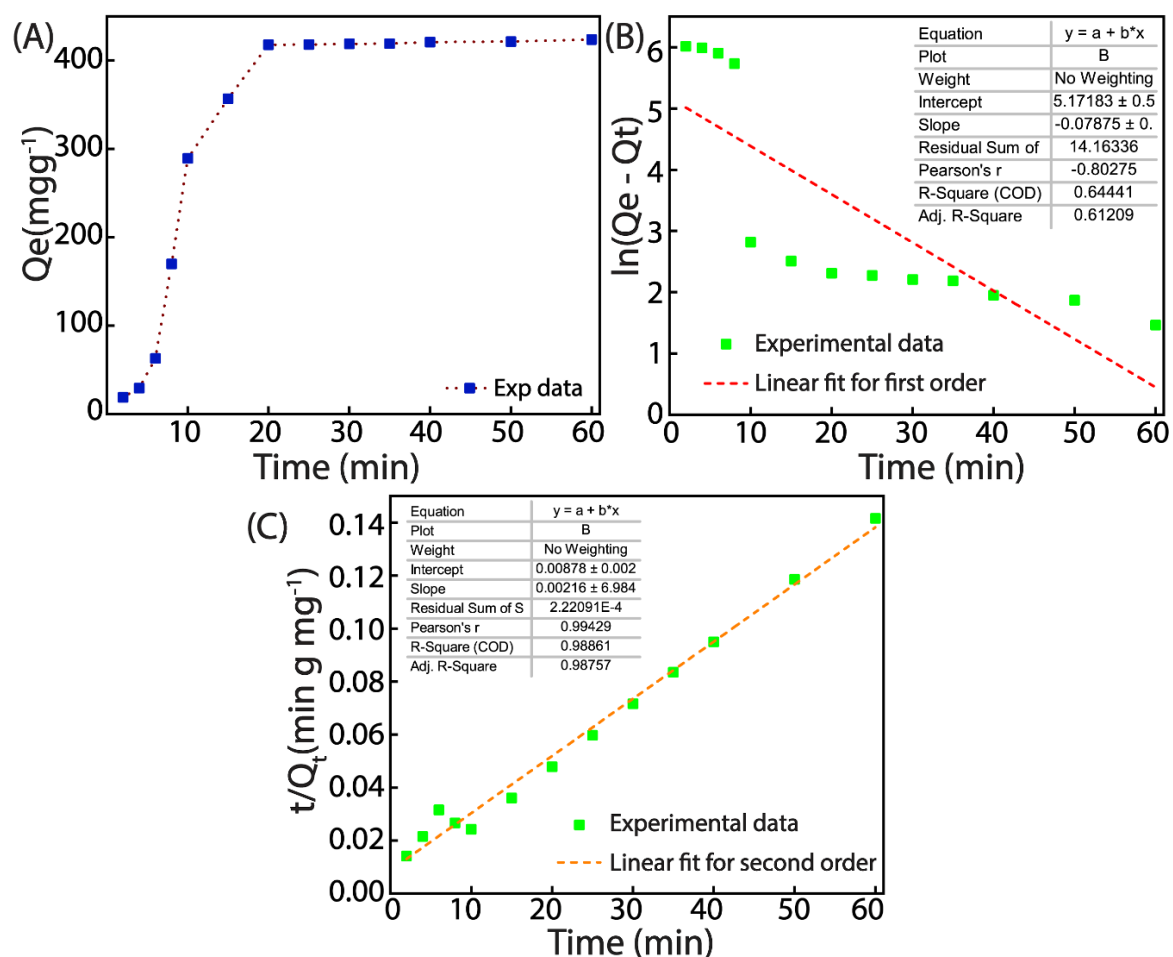


Fig. S26. Time-dependent desorption isotherm of arsenate by IC-CON (5mg) under room temperature (A), time-dependent desorption efficiency of IC-CON fitted with the first order (B) and second order (C) kinetics models.

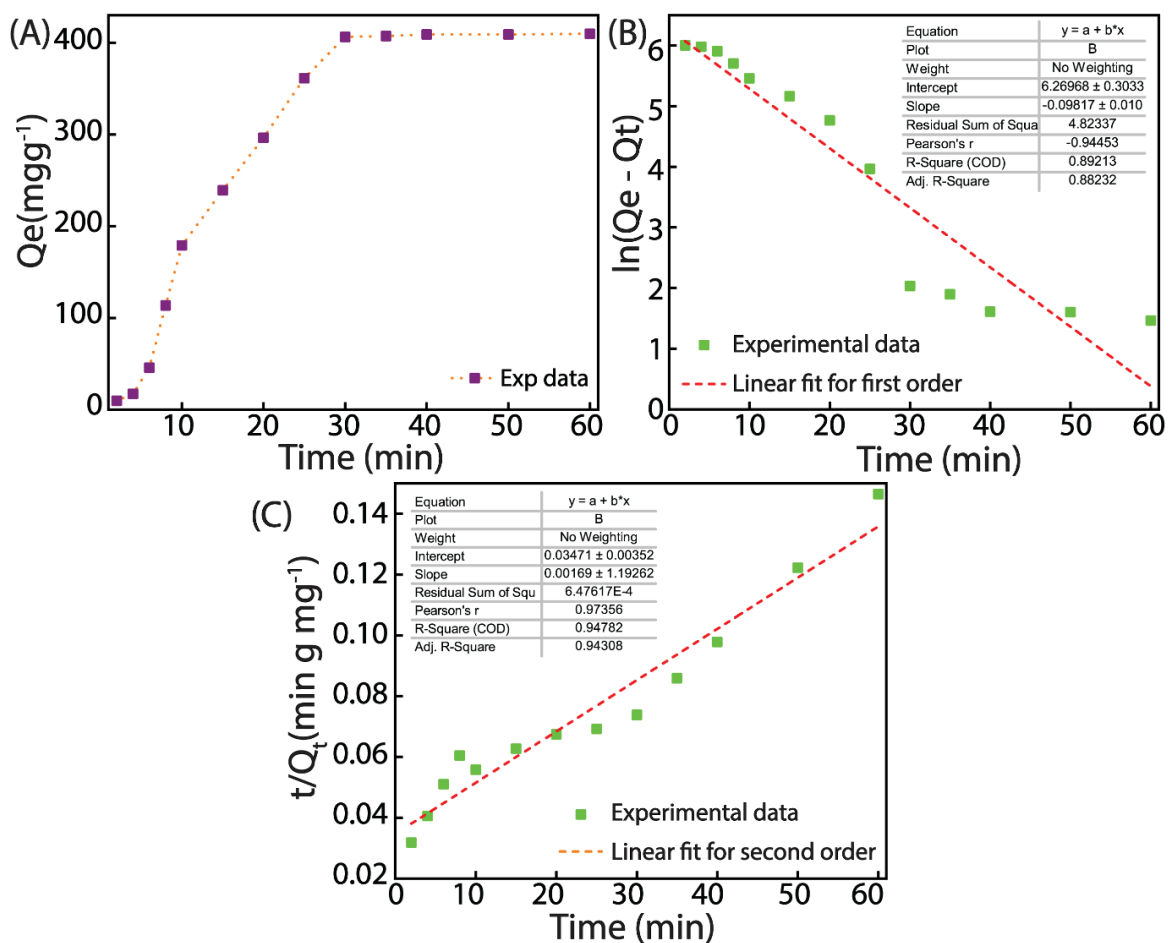


Fig. S27. Time-dependent desorption isotherm of phosphate by IC-CON (5mg) under room temperature (A), time-dependent desorption efficiency of IC-CON fitted with the first order (B) and second order (C) kinetics models.

Morphological analysis after arsenate and phosphate ions adsorption:

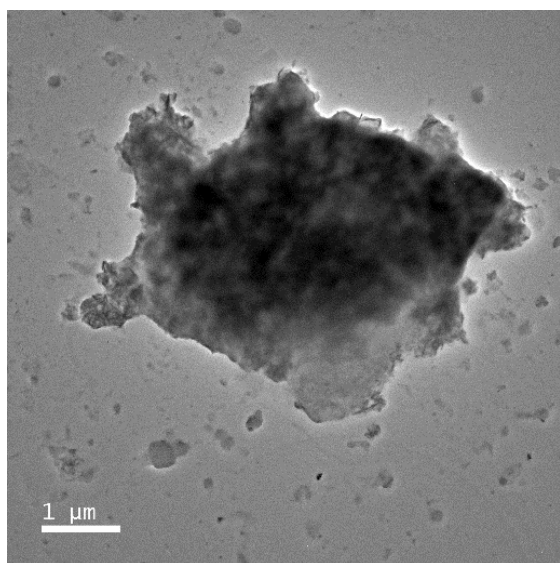


Fig. S28. FETEM Image after arsenate adsorption.

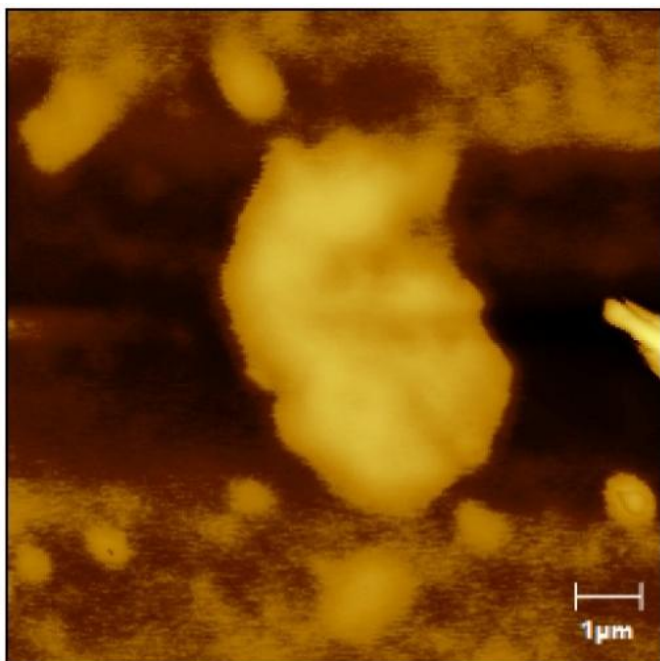


Fig. S29. AFM Image after arsenate adsorption.

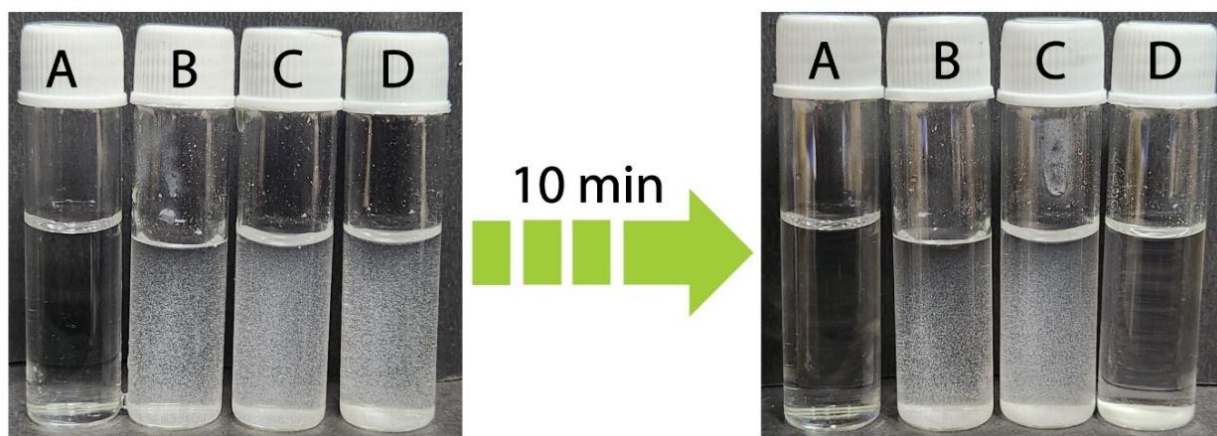


Fig. S30. Visual observation experiment of different adsorption patterns of arsenate and phosphate. Here, A represents blank Milli-Q water, B is IC-CON treated with phosphate, C is untreated IC-CON, and D is IC-CON treated with arsenate.

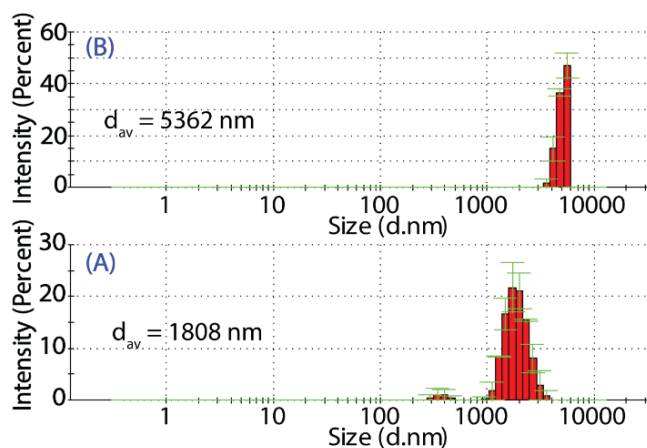


Fig. S31. DLS measurements of IC-CON polymer after treated with phosphate (A) and arsenate (B).

Mechanism for arsenate and phosphate adsorption:

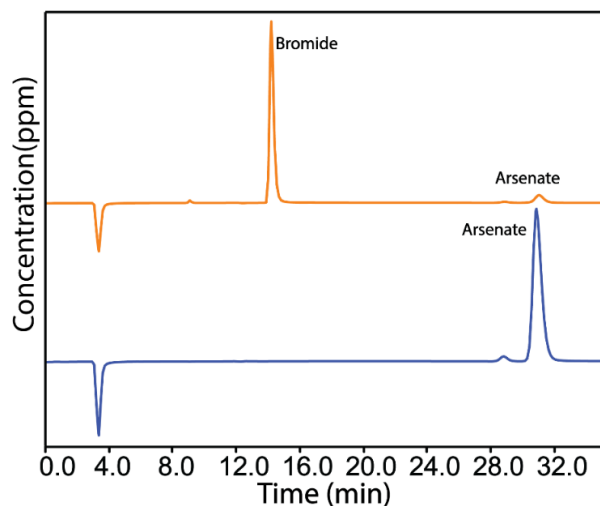


Fig. S32. IC spectra of arsenate solution before (blue) and after the treatment (orange) of IC-CON.

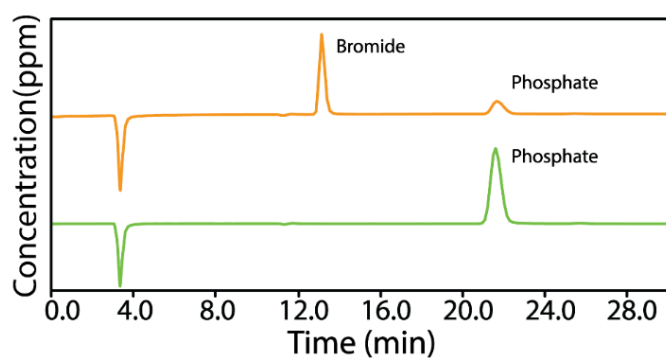


Fig. S33. IC spectra of phosphate solution before (green) and after the treatment (orange) of IC-CON.

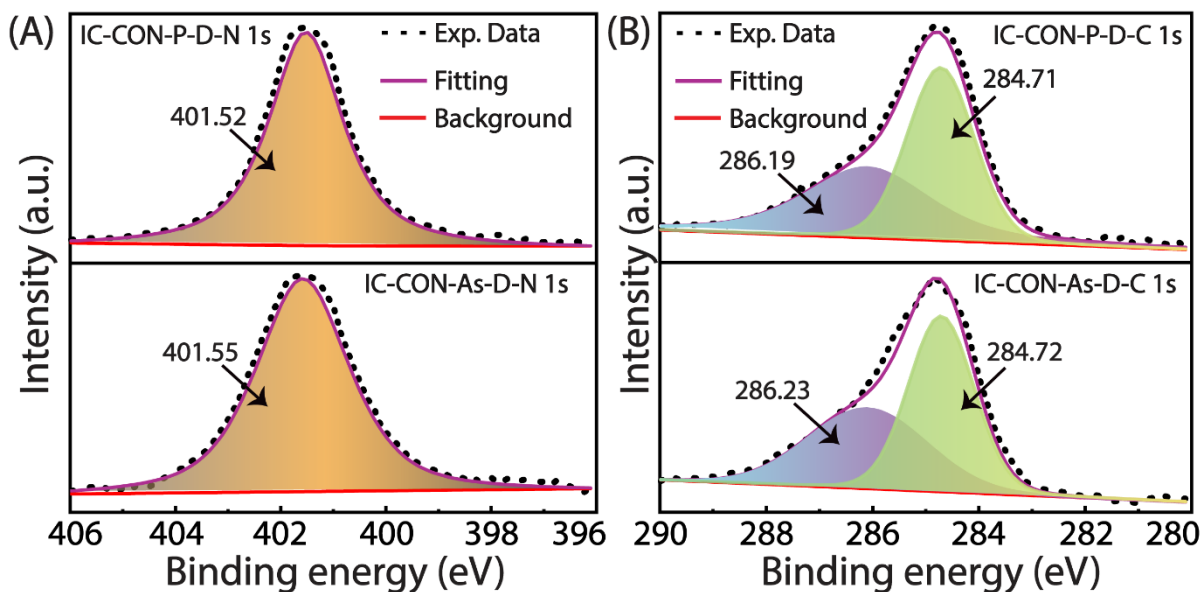


Fig. S34. Deconvoluted XPS spectra for the N 1s (A) and the C 1s (B) of IC-CON after the desorption of arsenate and phosphate ions.

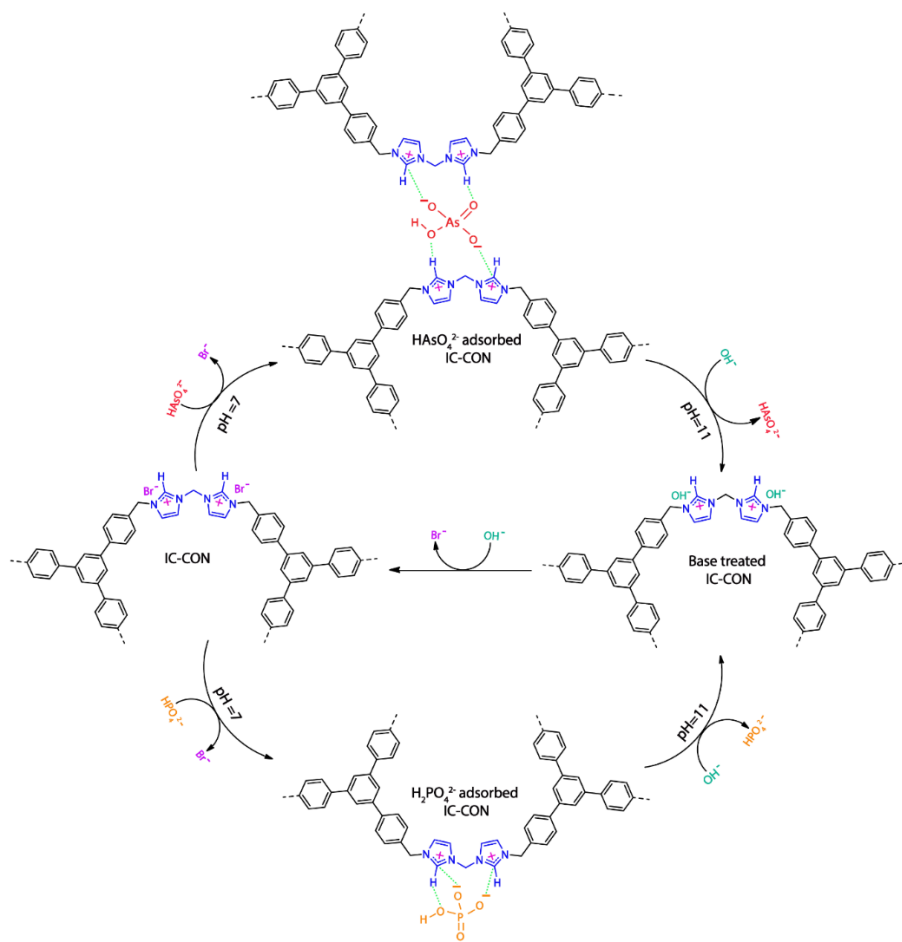


Fig. S35. Possible mechanistic pathways for adsorption and desorption process of arsenate and phosphate ions by IC-CON polymer.

Dynamic adsorption column experiment:

A glass column with an internal diameter of approximately 0.5 cm was employed for adsorption studies. The column was packed with 50 mg of IC-CON polymer and 3 g of sand, forming a bed of about 5 cm in length. Prior to conducting adsorption experiments, the column was preconditioned by passing 50 mL of ultrapure Milli-Q water to remove any trapped air.

The initial investigation focused on arsenate removal. A 0.5 ppm arsenate solution (500 mL), containing a ten-fold excess of competing anions (F^- , Cl^- , NO_3^- , CO_3^{2-} , and SO_4^{2-}), was introduced into the column in 10 mL batch at a flow rate of ~ 0.5 mL/min, with an equilibration time of 30 seconds. The eluates were collected in 10 fractions of 50 mL batch, and arsenate concentrations in each batch were analysed. The results showed that arsenate concentrations in the effluent remained below the World Health Organization (WHO) limit of 10 ppb for up to 350 mL of processed solution in the first cycle. To regenerate the column, 100 mL of 0.5N NaOH solution, followed by 50 mL of a 0.1 N NaBr solution was passed through, achieving over 96% desorption efficiency. The adsorption-desorption cycle was repeated five cycles, consistently yielding effluent arsenate concentrations below the WHO limit within 300 – 350 mL of treated solution in each cycle. The IC-CON polymer exhibited over 90% adsorbed arsenate removal efficiency per cycle, demonstrating its practical applicability.

Encouraged by the arsenate adsorption results, a similar methodology was applied for phosphate adsorption. A 50-ppm phosphate solution (500 mL), containing a ten-fold excess of competing anions (F^- , Cl^- , NO_3^- , CO_3^{2-} , and SO_4^{2-}), was passed through the column in 50 mL batch at a flow rate of ~ 0.5 mL/min, with an equilibration time of 1 minute. Analysis of the eluates showed that phosphate concentrations remained below the WHO threshold for up to 350 mL of treated solution. The column was then regenerated using 0.5 N NaOH, followed by 0.1 N NaBr as mentioned above, achieving over 94% phosphate desorption efficiency. The experiment was repeated for five cycles, with effluent phosphate concentrations consistently below the WHO limit within 250 – 350 mL of processed solution. The IC-CON polymer demonstrated over 87% phosphate removal efficiency per cycle.

To visually confirm the phosphate adsorption, two conical flasks containing 10 mL of ammonium molybdate tetrahydrate and concentrated nitric acid solution were taken. Two columns were set up: one containing IC-CON polymer and sand, and another with only sand. Equal volumes of a 50-ppm phosphate solution were passed through both columns, each with an equilibration time of 1 min. The effluent from the sand-packed column underwent a noticeable colour change from colourless to yellow, indicating the presence of phosphate ions.

In contrast, the effluent from the IC-CON polymer-packed column exhibited no colour change, signifying effective phosphate retention within the column.

The findings indicate that the IC-CON effectively removes arsenate and phosphate from aqueous solutions, even in the presence of competing anions. The polymer exhibited high adsorption efficiency over multiple cycles, with effective desorption during column regeneration. The visual detection tests further confirmed the adsorption capabilities of the polymer, highlighting its potential for real-world water treatment applications.

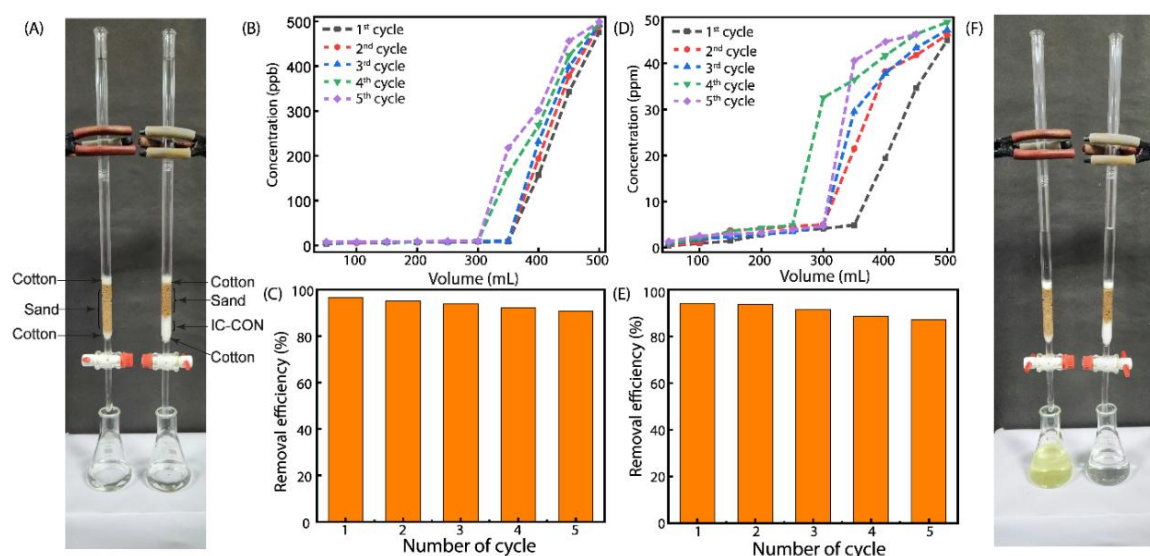


Fig. S36. Digital image for dynamic adsorption column experiment (A). Arsenate adsorption (B) and desorption (C) efficacy through the dynamic adsorption column experiment. Phosphate adsorption (D) and desorption (E) efficacy through the dynamic adsorption column experiment. Visual observation test for phosphate adsorption through the dynamic adsorption column experiment (F).

Table S1. Comparison of arsenate adsorption capacity by recently reported materials.

Sl No.	Compound	Adsorption Capacity (mg/g)	pH	Equilibrium Time	Recycle	Reference
1	IC-CON	698	7.0	1 min	0.5 N NaOH/NaBr	This Work
2	PAF-1-NMDG	94.2	4.0	NA	1 M HCl and 1M NaOH	²
3	PAF-1-NMDG	85.5	7.0	<10 s	1 M HCl and 1M NaOH	²
4	IRA743 Resin	46.7	7.0	4 h	1 M HCl and 1M NaOH	²
5	Fe ₂ O ₃ and MnO on Honeycomb Briquette Cinders	1.5	7.0	12 h	NA	³
6	MOF-808	24.8	4.0	50 min	0.5 M Na ₂ SO ₄	⁴
7	UiO-66	147.7	7.0	48 h	NA	⁵
8	Fe-BTC	12.3	4.0	10 min	NA	⁶
9	MIL-53 (Al)	106.5	8.0	50 h	-	⁷
10	Crosslinked NMDG and Poly(vinylbenzene chloride)	16.4	6.0	10 h	NA	⁸
11	Fe-treated Cellulose	33.2	7.0	10 h	8% alkaline solution	⁹
12	Fe-modified Activated Charcoal	51.3	6.0	24 h	NA	¹⁰
13	Fe(0) Nanoparticles on Chitosan	119	7.0	3 h	0.1 M NaOH	¹¹

14	Molybdate Chitosan Derivatives	230	2.0- 3.0	24 h	Sodium phosphate	12
15	H-MFI-90 Synthetic Zeolite	34.8	6.5	100 min	HCl (0.1 N) and NaOH (0.1 N)	13
16	H-MFI-24 Synthetic Zeolite	35.8	6.5	100 min	HCl (0.1 N) and NaOH (0.1 N)	13
17	Ultrafine Fe ₂ O ₃ Nanoparticles	47	7.0	2 h	NA	14
18	Poly(glycidyl methacrylate- <i>N</i> -methyl-D- glucamine)	45.9	3.0	NA	NA	15

NA = Not Available.

Table S2. Comparison of phosphate adsorption capacity by recently reported materials.

Sl No.	Compound	Adsorpti on Capacity (mg/g)	pH	Equili brium Time	Recycle	Refer ence
1	IC-CON	503	7	2 min	0.5 N NaOH/NaBr	This Work
2	ag-CON	719	6.0	<1 min	1 N NaOH	16
3	gCON	398	7.0	20 min	0.5 M NaOH	17
4	UiO-66	85	NA	2 h	0.01 M NaOH	18
5	UiO-66-NH ₂	92	NA	2 h	0.01 M NaOH	18
6	UiO-66	415	7.0	5 min	Dilute HNO ₃	19
7	Zr-loaded MIL-101	20.83	6.5	6 h	0.003 M NaOH	20
8	Zirconium cross linked graphene oxide/alginate	255.35	NA	7h	NA	21

9	ZrO ₂ functionalized graphite oxide	16.45	6.0	436 min	0.1 M NaOH	22
10	Zirconium-modified zeolite	10.2	7.0	24 h	NA	23
11	Zr/Al-pillared montmorillonite	17.2	5.0	6 h	NA	24
12	ZrO ₂ /SiO ₂ NM	43.8	5.0	30 min	0.1 M NaOH	25
13	Zr/PVA-modified PVDF membrane	21.64	7.0	30 h	NA	26
14	Zr-loaded orange waste gel	57	7.0	15 h	0.2 M NaOH	27
15	Zr-loaded wheat straw	31.9	NA	10 h	5 wt % NaOH + 5 wt % NaCl	28
16	ZrO ₂ loaded amine crosslinked shaddock Peel	59.89	3.0	4 h	NA	29
17	ZrO ₂ loaded lignocellulosic butanol residue	7.17	6.0	250 min	NA	30
18	Fe ₃ O ₄ @SiO ₂ @ZrO ₂	39.1	NA	5h	0.1 M KOH	31
19	Fe ₃ O ₄ @ZrO ₂	69.44	5.0	16 h	1 M NaOH	32
20	ZrO ₂ @SiO ₂ @Fe ₃ O ₄	6.33	7.0	60 min	0.1 M NaOH + 1 M Na ₂ SO ₄	33
21	ZrO ₂ @Fe ₃ O ₄	15.98	7.0	15 min	1 M NaOH	34
22	Zr-loaded collagen fiber	33.8	6.0	3 h	NA	35
23	Zirconium sulfate loaded polymer	110	7.0	2 h	NA	36
24	ZrO ₂ -loaded D-201	47.9	6.5	6 h	5 % NaOH + 5 % NaCl	37
25	ZrO ₂ -loaded IRA- 400	91.74	NA	NA	NA	38
26	Zirconium molybdate- loaded anion exchange	42.2	5.5	9 h	0.1 M NaOH	39
27	Zr (IV)-modified chitosan	47.44	7.0	20 min	NA	40

28	ZrO ₂ -loaded PANI	32.4	6.9	24 h	NA	41
29	Zr-loaded magnetic IPN hydrogel	50.76	6.5	20 h	0.05 M NaOH	41
30	MIP	78.88	NA	60 min	NA	42
31	ZnAl layered double hydroxide (ZnAlLDH)	57.05	NA	4 h	0.1 M NaOH	43
32	MCM-41	45.16	NA	10 min	NA	44
33	PMSB800	25.19	NA	24 h	NA	45
34	gCP	97	7.0	35-40 min	NaOH	46
35	Zn-gCP	310	7.0	20 min	NaOH	46
36	SA/Zr hydrogel	256.79	3.0	48 h	NA	47

NA = Not Available.

^1H and ^{13}C NMR spectra of synthesized compounds:

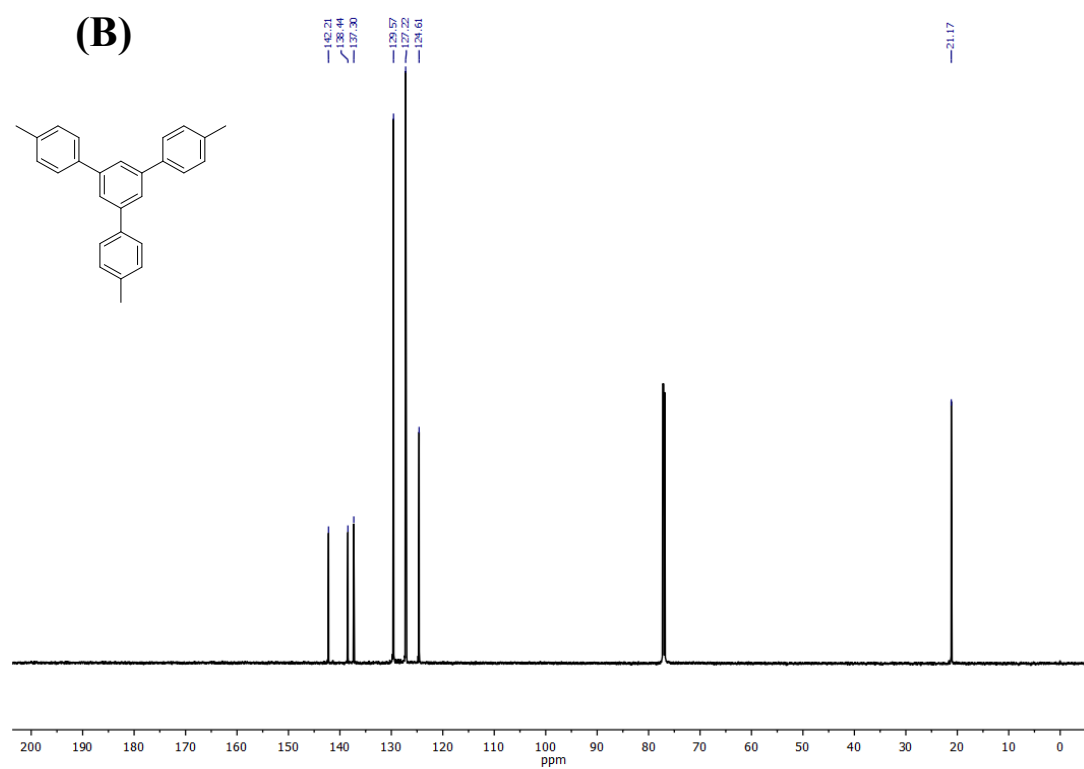
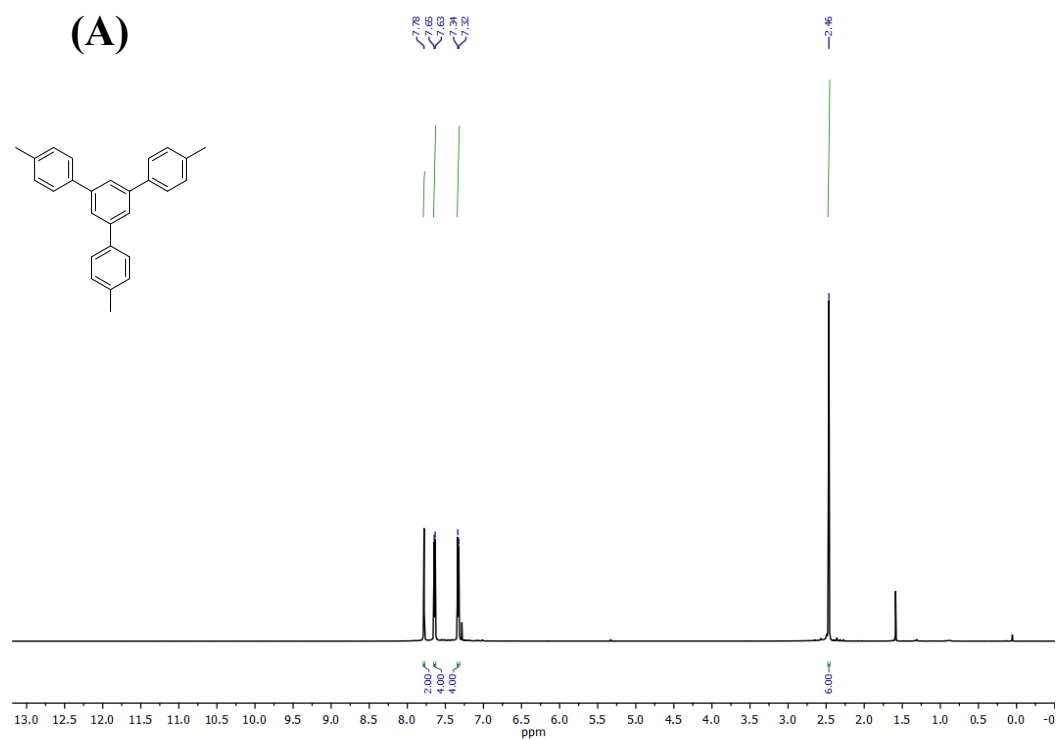


Fig. S37. ^1H (A) and ^{13}C (B) NMR spectra of 4,4'-dimethyl-5'-(p-tolyl)-1,1':3',1''-terphenyl.

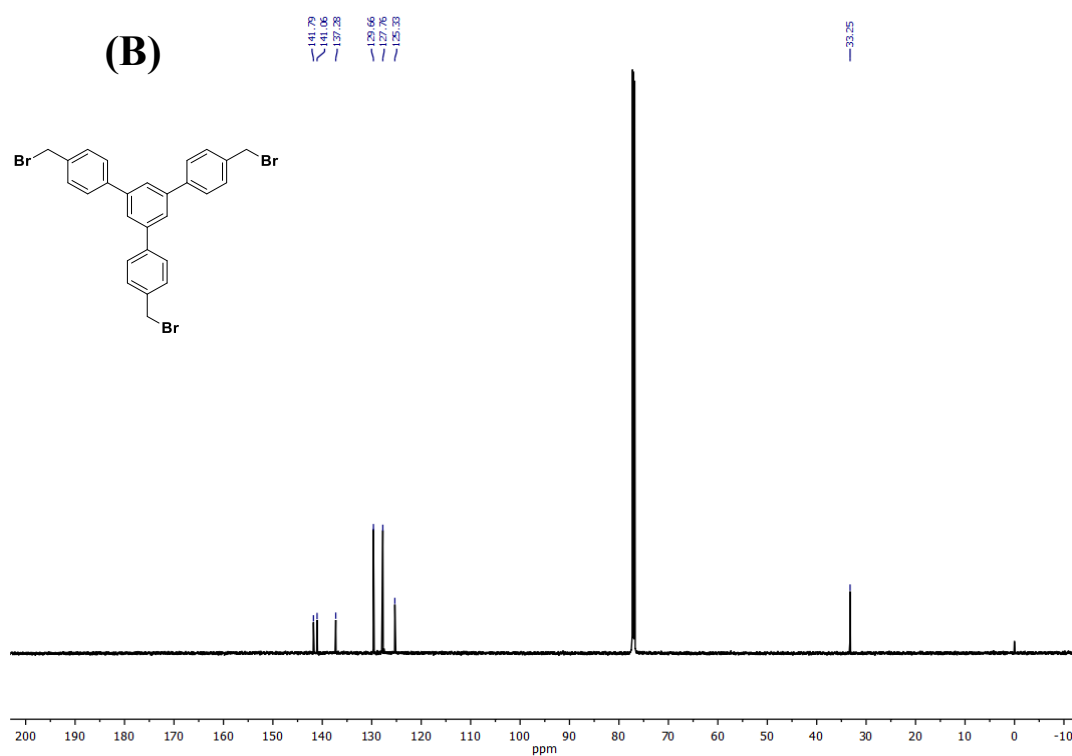
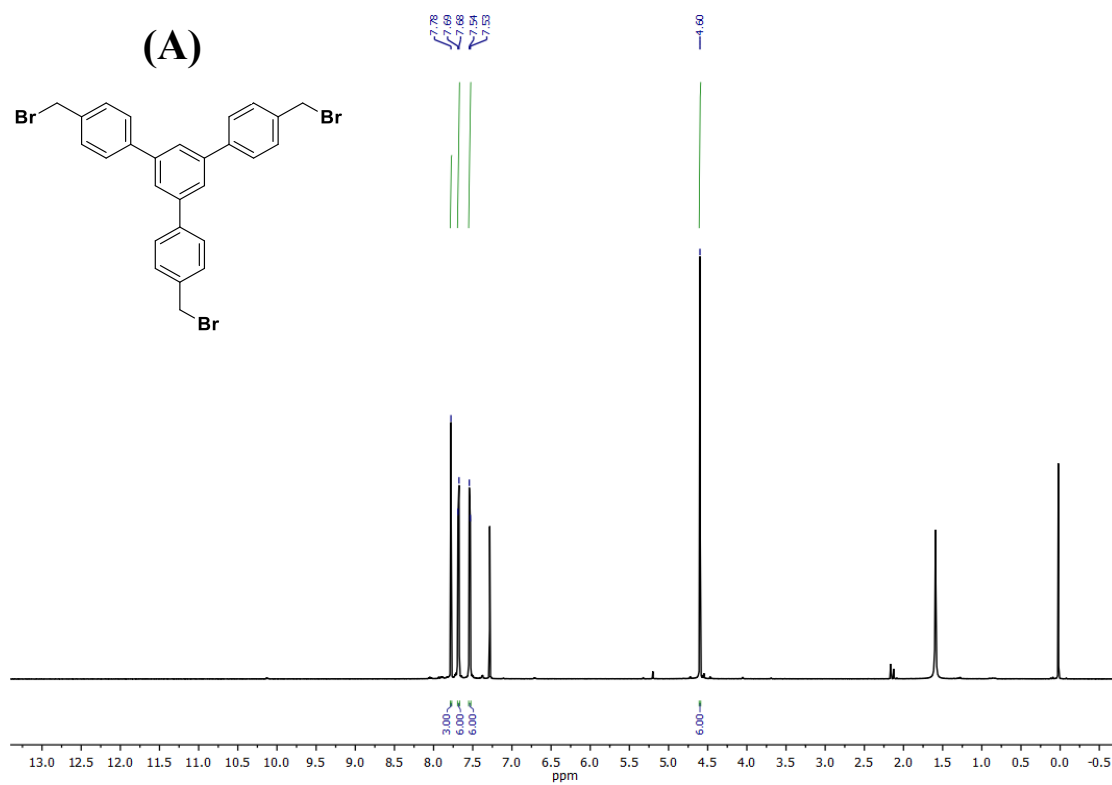


Fig. S38. ^1H (A) and ^{13}C (B) NMR spectra of 4,4'-bis(bromomethyl)-5'-(4-(bromomethyl)phenyl)-1,1'-biphenyl.

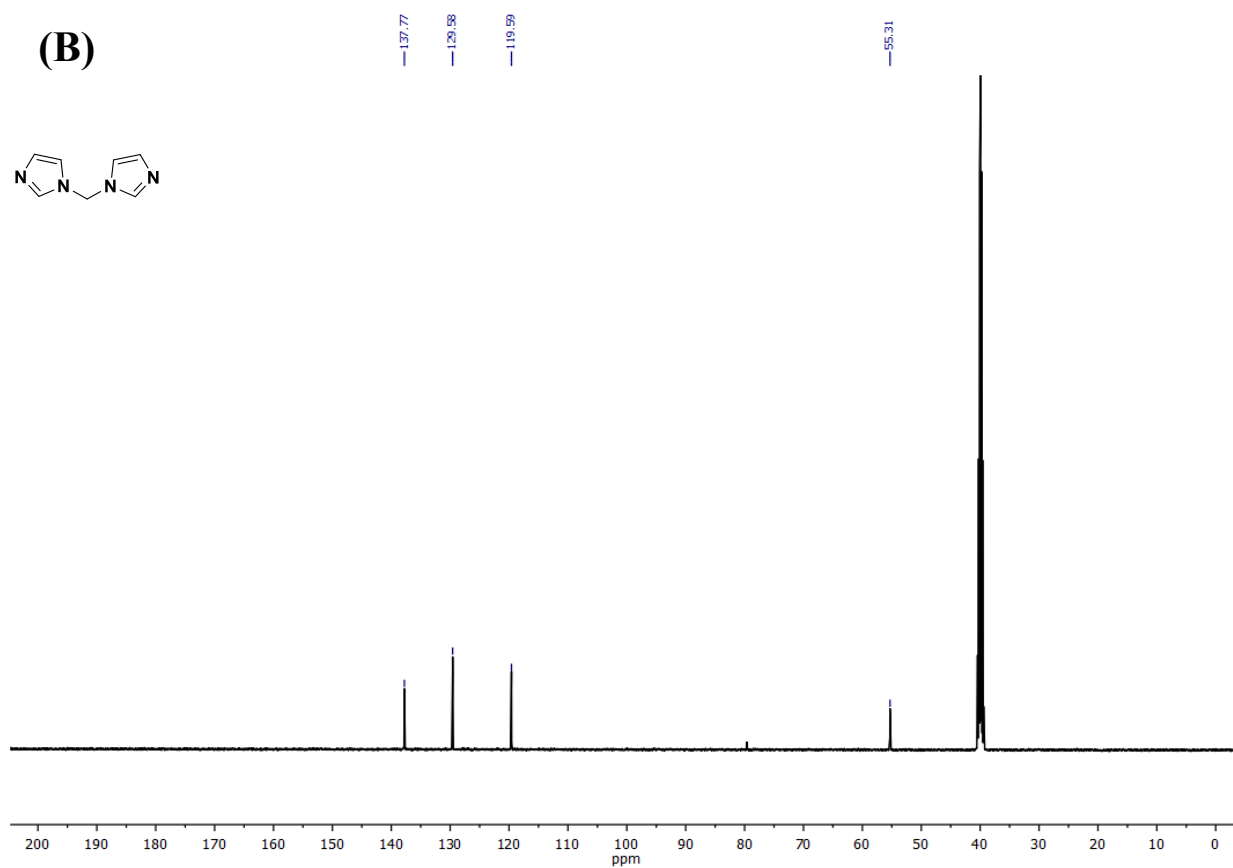
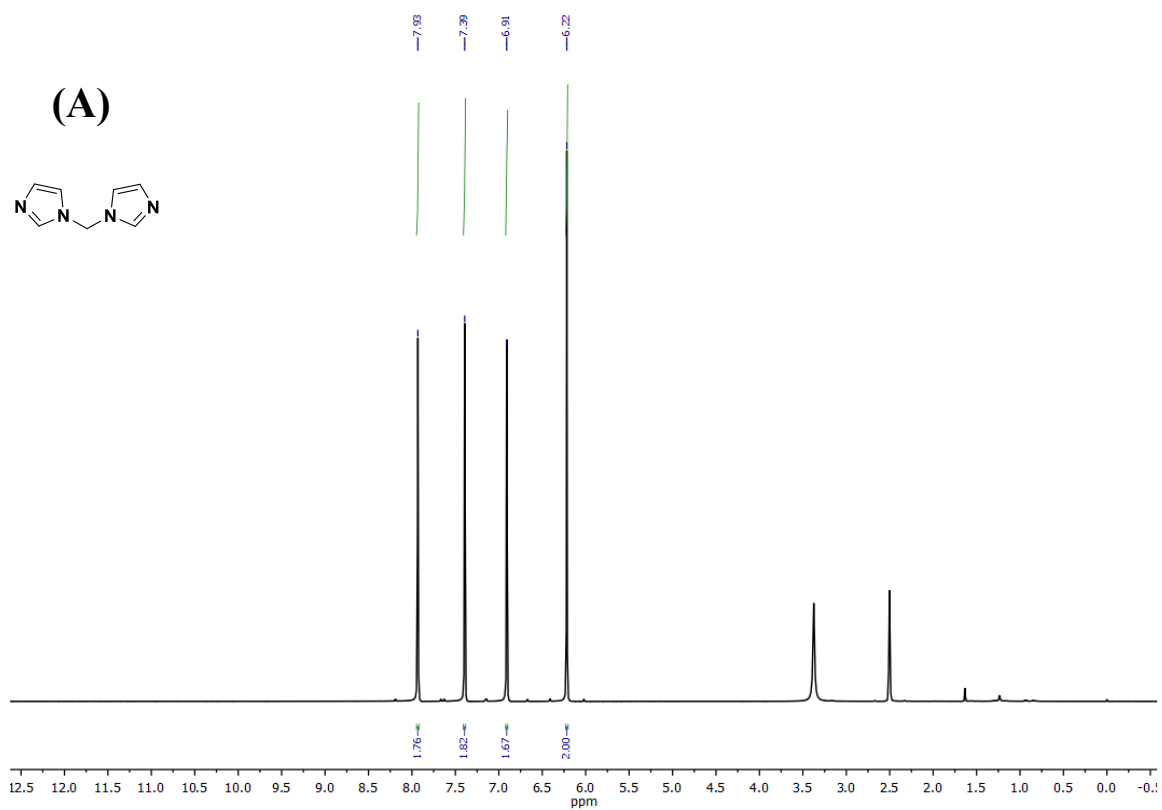


Fig. S39. ^1H (A) and ^{13}C (B) NMR spectra of di(1*H*-imidazol-1-yl)methane.

References:

1. Razavi, S. A. A.; Habibzadeh, E.; Morsali, A., High Capacity Arsenate Removal from Real Samples Using Dihydropyridazine Decorated Zirconium-Based Metal–Organic Frameworks. *ACS Appl. Mater. Interfaces* **2024**, *16* (10), 12573-12585.
2. Uliana, A. A.; Pezoulas, E. R.; Zakaria, N. I.; Johnson, A. S.; Smith, A.; Lu, Y.; Shaidu, Y.; Velasquez, E. O.; Jackson, M. N.; Blum, M., Removal of chromium and arsenic from water using polyol-functionalized porous aromatic frameworks. *J. Am. Chem. Soc.* **2024**, *146* (34), 23831-23841.
3. Zhu, J.; Baig, S. A.; Sheng, T.; Lou, Z.; Wang, Z.; Xu, X., Fe₃O₄ and MnO₂ assembled on honeycomb briquette cinders (HBC) for arsenic removal from aqueous solutions. *J. Hazard. Mater.* **2015**, *286*, 220-228.
4. Li, Z.-Q.; Yang, J.-C.; Sui, K.-W.; Yin, N., Facile synthesis of metal-organic framework MOF-808 for arsenic removal. *Mater. Lett.* **2015**, *160*, 412-414.
5. Wang, C.; Liu, X.; Chen, J. P.; Li, K., Superior removal of arsenic from water with zirconium metal-organic framework UiO-66. *Sci. Rep.* **2015**, *5* (1), 16613.
6. Zhu, B.-J.; Yu, X.-Y.; Jia, Y.; Peng, F.-M.; Sun, B.; Zhang, M.-Y.; Luo, T.; Liu, J.-H.; Huang, X.-J., Iron and 1, 3, 5-benzenetricarboxylic metal–organic coordination polymers prepared by solvothermal method and their application in efficient As (V) removal from aqueous solutions. *J. Phys. Chem. C* **2012**, *116* (15), 8601-8607.
7. Li, J.; Wu, Y.-n.; Li, Z.; Zhu, M.; Li, F., Characteristics of arsenate removal from water by metal-organic frameworks (MOFs). *Water Sci. Technol* **2014**, *70* (8), 1391-1397.
8. Dambies, L.; Salinaro, R.; Alexandratos, S. D., Immobilized N-methyl-D-glucamine as an arsenate-selective resin. *Environ. Sci. Technol.* **2004**, *38* (22), 6139-6146.
9. Guo, X.; Chen, F., Removal of arsenic by bead cellulose loaded with iron oxyhydroxide from groundwater. *Environ. Sci. Technol.* **2005**, *39* (17), 6808-6818.
10. Chen, W.; Parette, R.; Zou, J.; Cannon, F. S.; Dempsey, B. A., Arsenic removal by iron-modified activated carbon. *Water Res.* **2007**, *41* (9), 1851-1858.
11. Gupta, A.; Yunus, M.; Sankararamkrishnan, N., Zerovalent iron encapsulated chitosan nanospheres—A novel adsorbent for the removal of total inorganic Arsenic from aqueous systems. *Chemosphere* **2012**, *86* (2), 150-155.
12. Dambies, L.; Vincent, T.; Guibal, E., Treatment of arsenic-containing solutions using chitosan derivatives: uptake mechanism and sorption performances. *Water Res.* **2002**, *36* (15), 3699-3710.
13. Chutia, P.; Kato, S.; Kojima, T.; Satokawa, S., Arsenic adsorption from aqueous solution on synthetic zeolites. *J. Hazard. Mater.* **2009**, *162* (1), 440-447.
14. Tang, W.; Li, Q.; Gao, S.; Shang, J. K., Arsenic (III, V) removal from aqueous solution by ultrafine α -Fe₂O₃ nanoparticles synthesized from solvent thermal method. *J. Hazard. Mater.* **2011**, *192* (1), 131-138.
15. Toledo, L.; Rivas, B. L.; Urbano, B. F.; Sánchez, J., Novel N-methyl-D-glucamine-based water-soluble polymer and its potential application in the removal of arsenic. *Sep. Purif. Technol.* **2013**, *103*, 1-7.
16. Hazarika, G.; Das, S.; Das, N. M.; Manna, D., A pH-responsive covalent organic network: Morphology change leads to capture and removal of phosphate ions from water. *J Mater Chem A* **2024**, *12* (30), 19559-19566.
17. Dey, S.; Das, S.; Patel, A.; Raj, K. V.; Vanka, K.; Manna, D., Antimicrobial two-dimensional covalent organic nanosheets (2D-CONs) for the fast and highly efficient capture and recovery of phosphate ions from water. *J Mater Chem A.* **2022**, *10* (9), 4585-4593.
18. Lin, K.-Y. A.; Chen, S.-Y.; Jochems, A. P.; Physics, Zirconium-based metal organic frameworks: Highly selective adsorbents for removal of phosphate from water and urine. *Mater. Chem. Phys.* **2015**, *160*, 168-176.
19. Gu, Y.; Xie, D.; Ma, Y.; Qin, W.; Zhang, H.; Wang, G.; Zhang, Y.; Zhao, H., Size modulation of zirconium-based metal organic frameworks for highly efficient phosphate remediation. *ACS Appl. Mater. Interfaces.* **2017**, *9* (37), 32151-32160.

20. Liu, T.; Feng, J.; Wan, Y.; Zheng, S.; Yang, L., ZrO₂ nanoparticles confined in metal organic frameworks for highly effective adsorption of phosphate. *Chemosphere* **2018**, *210*, 907-916.
21. Shan, S.; Tang, H.; Zhao, Y.; Wang, W.; Cui, F., Highly porous zirconium-crosslinked graphene oxide/alginate aerogel beads for enhanced phosphate removal. *Chem. Eng. J.* **2019**, *359*, 779-789.
22. Zong, E.; Wei, D.; Wan, H.; Zheng, S.; Xu, Z.; Zhu, D., Adsorptive removal of phosphate ions from aqueous solution using zirconia-functionalized graphite oxide. *Chem. Eng. J.* **2013**, *221*, 193-203.
23. Yang, M.; Lin, J.; Zhan, Y.; Zhu, Z.; Zhang, H., Immobilization of phosphorus from water and sediment using zirconium-modified zeolites. *Environ. Sci. Pollut. R.* **2015**, *22*, 3606-3619.
24. Huang, W.; Chen, J.; He, F.; Tang, J.; Li, D.; Zhu, Y.; Zhang, Y., Effective phosphate adsorption by Zr/Al-pillared montmorillonite: insight into equilibrium, kinetics and thermodynamics. *Appl. Clay. Sci.* **2015**, *104*, 252-260.
25. Wang, X.; Dou, L.; Li, Z.; Yang, L.; Yu, J.; Ding, B., Flexible hierarchical ZrO₂ nanoparticle-embedded SiO₂ nanofibrous membrane as a versatile tool for efficient removal of phosphate. *ACS Appl. Mater. Interfaces* **2016**, *8* (50), 34668-34676.
26. Zhao, D.; Chen, J. P., Application of zirconium/PVA modified flat-sheet PVDF membrane for the removal of phosphate from aqueous solution. *Ind. Eng. Chem. Res.* **2016**, *55* (24), 6835-6844.
27. Biswas, B. K.; Inoue, K.; Ghimire, K. N.; Harada, H.; Ohto, K.; Kawakita, H., Removal and recovery of phosphorus from water by means of adsorption onto orange waste gel loaded with zirconium. *Bioresource Technol.* **2008**, *99* (18), 8685-8690.
28. Qiu, H.; Liang, C.; Zhang, X.; Chen, M.; Zhao, Y.; Tao, T.; Xu, Z.; Liu, G., Fabrication of a biomass-based hydrous zirconium oxide nanocomposite for preferable phosphate removal and recovery. *ACS Appl. Mater. Interfaces.* **2015**, *7* (37), 20835-20844.
29. Duan, P.; Xu, X.; Shang, Y.; Gao, B.; Li, F., Amine-crosslinked Shaddock Peel embedded with hydrous zirconium oxide nano-particles for selective phosphate removal in competitive condition. *J. Taiwan Inst. Chem. E.* **2017**, *80*, 650-662.
30. Zong, E.; Liu, X.; Jiang, J.; Fu, S.; Chu, F., Preparation and characterization of zirconia-loaded lignocellulosic butanol residue as a biosorbent for phosphate removal from aqueous solution. *Appl. Surf. Sci.* **2016**, *387*, 419-430.
31. Sarkar, A.; Biswas, S. K.; Pramanik, P., Design of a new nanostructure comprising mesoporous ZrO₂ shell and magnetite core (Fe₃O₄@mZrO₂) and study of its phosphate ion separation efficiency. *J. Mater. Chem.* **2010**, *20* (21), 4417-4424.
32. Wang, Z.; Xing, M.; Fang, W.; Wu, D., One-step synthesis of magnetite core/zirconia shell nanocomposite for high efficiency removal of phosphate from water. *Appl. Surf. Sci.* **2016**, *366*, 67-77.
33. Fang, L.; Wu, B.; Lo, I. M., Fabrication of silica-free superparamagnetic ZrO₂@Fe₃O₄ with enhanced phosphate recovery from sewage: performance and adsorption mechanism. *Chem. Eng. J.* **2017**, *319*, 258-267.
34. Liao, X.-P.; Ding, Y.; Wang, B.; Shi, B., Adsorption behavior of phosphate on metal-ions-loaded collagen fiber. *Ind. Eng. Chem. Res.* **2006**, *45* (11), 3896-3901.
35. Pitakteeratham, N.; Hafuka, A.; Satoh, H.; Watanabe, Y., High efficiency removal of phosphate from water by zirconium sulfate-surfactant micelle mesostructure immobilized on polymer matrix. *Water Res.* **2013**, *47* (11), 3583-3590.
36. Chen, L.; Zhao, X.; Pan, B.; Zhang, W.; Hua, M.; Lv, L.; Zhang, W., Preferable removal of phosphate from water using hydrous zirconium oxide-based nanocomposite of high stability. *J. Hazard. Mater.* **2015**, *284*, 35-42.
37. Acelas, N. Y.; Martin, B. D.; López, D.; Jefferson, B., Selective removal of phosphate from wastewater using hydrated metal oxides dispersed within anionic exchange media. *Chemosphere* **2015**, *119*, 1353-1360.
38. Bui, T. H.; Hong, S. P.; Yoon, J., Development of nanoscale zirconium molybdate embedded anion exchange resin for selective removal of phosphate. *Water Res.* **2018**, *134*, 22-31.
39. Liu, Q.; Hu, P.; Wang, J.; Zhang, L.; Huang, R., Phosphate adsorption from aqueous solutions by Zirconium (IV) loaded cross-linked chitosan particles. *J. Taiwan. Inst. Chem. E.* **2016**, *59*, 311-319.

40. Masim, F. C. P.; Tsai, C.-H.; Lin, Y.-F.; Fu, M.-L.; Liu, M.; Kang, F.; Wang, Y.-F., Synergistic effect of PANI–ZrO₂ composite as antibacterial, anti-corrosion, and phosphate adsorbent material: synthesis, characterization and applications. *Environ. Technol.* **2019**, *40* (2), 226-238.
41. Wan, J.; Zhu, C.; Hu, J.; Zhang, T. C.; Richter-Egger, D.; Feng, X.; Zhou, A.; Tao, T., Zirconium-loaded magnetic interpenetrating network chitosan/poly (vinyl alcohol) hydrogels for phosphorus recovery from the aquatic environment. *Appl. Surf. Sci.* **2017**, *423*, 484-491.
42. Xi, Y.; Huang, M.; Luo, X., Enhanced phosphate adsorption performance by innovative anion imprinted polymers with dual interaction. *Appl. Surf. Sci.* **2019**, *467*, 135-142.
43. Yu, Q.; Zheng, Y.; Wang, Y.; Shen, L.; Wang, H.; Zheng, Y.; He, N.; Li, Q., Highly selective adsorption of phosphate by pyromellitic acid intercalated ZnAl-LDHs: assembling hydrogen bond acceptor sites. *Chem. Eng. J.* **2015**, *260*, 809-817.
44. Choi, J.-W.; Lee, S.-Y.; Chung, S.-G.; Hong, S.-W.; Kim, D.-J.; Lee, S.-H., Removal of phosphate from aqueous solution by functionalized mesoporous materials. *Water Air Soil Poll.* **2011**, *222*, 243-254.
45. Zhang, M.; Lin, K.; Li, X.; Wu, L.; Yu, J.; Cao, S.; Zhang, D.; Xu, L.; Parikh, S. J.; Ok, Y. S., Removal of phosphate from water by paper mill sludge biochar. *Environ. Pollut.* **2022**, *293*, 118521.
46. Hazarika, G.; Das, S.; Patel, A.; Manna, D., Guanidine-modified cellulose enhances capturing and recovery of phosphates from wastewater. *Environ. Sci.: Water Res. Technol.* **2025**.
47. Qing, Z.; Wang, L.; Liu, X.; Song, Z.; Qian, F.; Song, Y. J. C., Simply synthesized sodium alginate/zirconium hydrogel as adsorbent for phosphate adsorption from aqueous solution: Performance and mechanisms. *Chemosphere* **2022**, *291*, 133103.